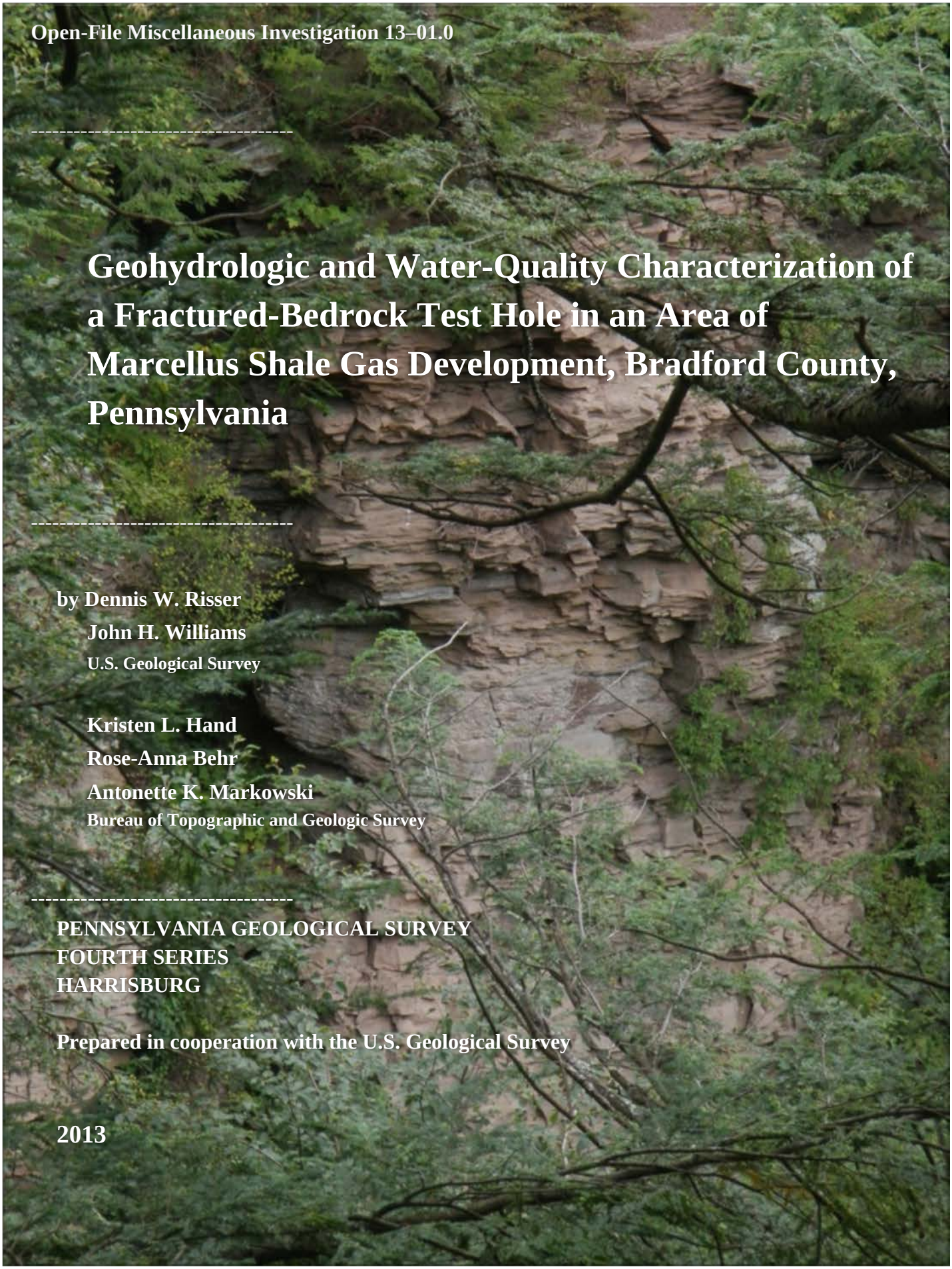

Open-File Miscellaneous Investigation 13–01.0

Geohydrologic and Water-Quality Characterization of a Fractured-Bedrock Test Hole in an Area of Marcellus Shale Gas Development, Bradford County, Pennsylvania

---

by Dennis W. Risser
John H. Williams
U.S. Geological Survey

Kristen L. Hand
Rose-Anna Behr
Antonette K. Markowski
Bureau of Topographic and Geologic Survey

PENNSYLVANIA GEOLOGICAL SURVEY
FOURTH SERIES
HARRISBURG

Prepared in cooperation with the U.S. Geological Survey

2013

OPEN-FILE REPORT DISCLAIMER

No Warranty

This open-file report and accompanying documentation are provided "as is," and the user assumes the entire risk as to their quality and performance.

The Commonwealth of Pennsylvania makes no guarantee or warranty concerning the accuracy of information contained in the geographic data or accompanying documentation. The Commonwealth of Pennsylvania further makes no warranties, either expressed or implied, as to any other matter whatsoever, including, without limitation, the completeness or condition of the product, or its fitness for any particular purpose. The burden for determining fitness for use lies entirely with the user.

Although the text and images have been processed successfully on a computer system at the Bureau of Topographic and Geologic Survey, the Commonwealth of Pennsylvania makes no warranty, expressed or implied, regarding the use of the report or accompanying documentation on any other computer system, nor does the act of distribution constitute any such warranty.

Limitation of Liability

The user shall save the Commonwealth of Pennsylvania harmless from any suits, claims, or actions arising out of the use of or any defect in the open-file report or accompanying documentation.

The Commonwealth of Pennsylvania assumes no legal liability for the accuracy, completeness, or usefulness of the open-file report and accompanying documentation. In no event shall the Commonwealth of Pennsylvania have any liability whatsoever for payment of any consequential, incidental, indirect, special, or tort damages of any kind, including, but not limited to, any loss of profits arising out of use of or reliance on the geographic or geologic data.

Use and Access Constraints

Not for commercial resale.

This open-file report is not designed for use as a primary regulatory tool in permitting and siting decisions. It is public information and, as such, it may be used as a reference source and may be interpreted by organizations, agencies, units of government, or others based on needs; however, each user is responsible for the appropriate application of the data. Federal, state, or local regulatory bodies are not to reassign to the Bureau of Topographic and Geologic Survey any authority for the decisions they make using this report.

Endorsements

The use of trade, product, or firm names in this report is for descriptive purposes only and does not imply endorsement by the authors or their employers.

Material from this report may be published if credit is given to the
Pennsylvania Geological Survey

This report has been prepared in accordance with
the open-file reporting standards of the
Bureau of Topographic and Geologic Survey.
It has undergone external peer review through the U.S. Geological Survey in accordance
with their fundamental science practices.

ACKNOWLEDGMENT

This report was funded in part by the
USGS National Cooperative Geologic Mapping Program
USGS Cooperative Agreement G11AC20364
USGS Toxics Substances Hydrology Program

This open-file report can be obtained through
the Bureau of Topographic and Geologic Survey website at
www.dcnr.state.pa.us/topogeo/index.aspx

Suggested citation: Risser, D. W., Williams, J. H., Hand, K. L., and others, 2013, Geohydrologic and water-quality characterization of a fractured-bedrock test hole in an area of Marcellus shale gas development, Bradford County, Pennsylvania: Pennsylvania Geological Survey, 4th ser., Open-File Report OFMI 13–01.0, 49 p., 4 appendices.

CONTENTS

Abstract 9
Introduction 11
  Study Site And Test Hole 11
  Methods 11
    Core 12
    Geophysical Logs 13
    Water-Quality Samples 17
Geohydrologic And Water-Quality Characterization Of The Gleason Test Hole 19
  Spatial Trajectory Of The Test Hole 19
  Stratigraphy And Lithology 19
    Bedding 22
    Fractures 22
  Water-Bearing Zones 24
  Water Quality 31
    Specific Conductance, Dissolved Solids, And Major Ions 31
    Trace Constituents And Radiochemicals 34
    Organic Constituents And Nutrients 36
  Gases And Stable Isotopes 37
    Composition Of Gas Extracted From Core 37
    Concentrations Of Dissolved Gas And Stable Isotopes In Water 39
  Insights Into Active And Restricted Groundwater Flow 41
  Summary 43
Acknowledgments 45

ILLUSTRATIONS

FIGURES

Figure 1. Location of the Gleason test hole in the Tioga River watershed of Tioga and Bradford Counties, Pennsylvania. The Blossburg Syncline is northwest of the test hole location and plunges to the southwest (Faill, 2011; McLaurin and Dodge, 2012; Behr and Hand, 2013). Inset map shows location within the state. Base map is ESRI Topographic base map.. 11
Figure 2. The angle of the test hole from vertical generally increased with depth ranging up to 1.5 degrees near its bottom.. 18
Figure 3. Logs of stratigraphy, lithology, natural gamma, neutron porosity, density, and bedding orientation for the Gleason test hole, Bradford County, Pennsylvania. (explanation of log headings, units, and symbols are presented on page 7) 19
Figure 4. Devonian decapod, species currently unknown and under scientific review, present at a depth of 502.2 feet bls in the core from the Gleason test hole, Bradford County, Pennsylvania; specimen currently located in the Carnegie Museum collection. 20
Figure 5. Core sample of the carbonaceous layer seen within the Huntley Mountain Formation at 255 feet bls and sent for gas isotope analysis, Gleason test hole, Bradford County, Pennsylvania. 20
Figure 6. Gamma and lithologic logs and acoustic and optical televiewer images of carbonaceous zone penetrated at 1310 feet bls by the Gleason test hole, Bradford County, Pennsylvania (explanation of log headings, units, and symbols are presented on page 7). 21
Figure 7. Lower-hemisphere, equal-area projection of poles for bedding orientations penetrated by the Gleason test hole, Bradford County, Pennsylvania. 21

Figure 8. Stratigraphy, lithology with natural gamma and neutron, sonic amplitude and travel time, and caliper logs and of breakout and fracture orientation for the Gleason test hole, Bradford County, Pennsylvania (explanation of log headings, units, and symbols are presented on page 7).. 22
Figure 9. Cumulative frequency of penetrated fractures in relation to depth below land surface in the Gleason test hole, Bradford County, Pennsylvania. 23
Figure 10. Lower-hemisphere, equal-area projection of poles for fractures penetrated by the Gleason test hole, Bradford County, Pennsylvania. 23
Figure 11. Logs showing stratigraphy, lithology, fluid resistivity, flow, temperature, fluid specific conductance, breakout orientation, and water-bearing fracture orientation and density for the Gleason test hole, Bradford County, Pennsylvania (Explanation of log headings, units, and symbols are presented on page). 24
Figure 12. Core photograph and acoustic and optical televiewer images of three steeply dipping fractures and a subhorizontal fracture penetrated at about 294 feet below land surface by the Gleason test hole, Bradford County, Pennsylvania. 25
Figure 13. Video still image from July 17, 2012 showing cascading water and inflow jetting in from a subhorizontal fracture at 249 feet below land surface in the Gleason test hole, Bradford County, Pennsylvania (video presented in Appendix 4). 25
Figure 14. Video still images from October 2, 2012 showing filamentous bacteria growth near a high angle fracture at the water-bearing zone 294 feet below land surface in the Gleason test hole, Bradford County, Pennsylvania (videos presented in Appendix 4). 25
Figure 15. Core photograph and acoustic and optical televiewer images of subhorizontal fracture penetrated at 553 feet below land surface along a sandstone-claystone contact by the Gleason test hole, Bradford County, Pennsylvania. 26
Figure 16. Core photograph and acoustic and optical televiewer images of a subhorizontal fracture penetrated at 661 feet below land surface by the Gleason test hole, Bradford County, Pennsylvania. 26
Figure 17. Video still image from October 2, 2012 showing freshwater outflow of rust-colored particles into a subhorizontal fracture penetrated at 661 feet below land surface by the Gleason test hole, Bradford County, Pennsylvania (videos presented in Appendix 4). 27
Figure 18. Core photograph, acoustic, and optical televiewer images of subhorizontal fracture penetrated at 712 feet below land surface by the Gleason test hole, Bradford County, Pennsylvania. 28
Figure 19. Core photograph and acoustic and optical televiewer images of subhorizontal fracture penetrated at about 1,026 feet below land surface by the Gleason test hole, Bradford County, Pennsylvania. 28
Figure 20. Video still images showing seepage of high-density saline water from subhorizontal fractures (A) at 914 below land surface on July 17, 2012 and (B) at 1,026 feet below land surface on October 2, 2012 in the Gleason test hole, Bradford County, Pennsylvania (videos presented in Appendix 4). 28
Figure 21. Logs of stratigraphy, lithology, gamma, neutron and density porosity, induction resistivity, and estimated formation water resisitivity for selected sandstone intervals penetrated by the Gleason test hole, Bradford County, Pennsylvania (explanation of log headings, units, and symbols are presented on p. 7). 29
Figure 22. Total dissolved-solids concentration and designation of salinity of the water for point samples collected at selected depths in the Gleason test hole, Bradford County, Pennsylvania. Circles represent the June 19-20, 2012 samples and the square represents the July 25, 2012 sample. Definitions of fresh and saline water are from U.S.Geological Survey (2012). 31
Figure 23. Trilinear diagram depicting the major-ion composition of five depth-dependent water samples collected from the Gleason test hole, Bradford County, Pennsylvania. 23
Figure 24. Concentrations of metals and other trace constituents in water sampled from specific depths in the Gleason test hole, Bradford County, Pennsylvania (non-detects for a few constituents are shown as half the detection level). 33
Figure 25. Relation between bromide and chloride concentrations in depth-dependent samples from the Gleason test hole, Bradford County, Pennsylvania. 35
Figure 26. Ratios of methane to higher chain hydrocarbon gases from samples of rock core and water samples collected at various depths in the Gleason test hole, Bradford County, Pennsylvania. 37
Figure 27. Stable carbon and hydrogen isotopic ratios for methane extracted from a carbonaceous zone in the rock core and from four specific-depth water samples in the Gleason test hole, Bradford County, Pennsylvania. Designated thermogenic, microbial, and fermentation origin fields from Breen and others (2007), modified from Coleman and others (1993). 38
Figure 28. Relation between sample depth and δ13C values for methane and ethane in groundwater and from a carbonaceous zone in the rock core at 1,310 feet below land surface in the Gleason test hole, Bradford County, Pennsylvania 39
Figure 29. Schematic diagram showing altitudes of water-bearing zones and altitudes of stream drainage in the vicintiy of the Gleason test hole, Bradford County, Pennsylvania. 41

TABLES

Table 1. Types of geophysical logs and dates of collection from the Gleason test hole, Bradford County, Pennsylvania..... 14
Table 2 Depth-dependent water-quality samples collected and constituents analyzed in groundwater from the Gleason test hole, Bradford County, Pennsylvania. 18
Table 3 Depths and description of samples taken from core BRA015-0204, Bradford County, Pennsylvania..... 38

CONVERSION FACTORS

Inch/Pound to SI

Multiply	By	To obtain
	Length	
inch (in.)	2.54	centimeter (cm)
foot (ft)	0.3048	meter (m)
mile (mi)	1.609	kilometer (km)
	Volume	
gallon (gal)	3.785	liter (L)
cubic foot (ft^3)	0.02832	cubic meter (m^3)
	Flow rate	
pound per square inch (lb/in^2)	6.895	kilopascal (kPa)
	Density	
pound per cubic foot (lb/ft^3)	0.01602	gram per cubic centimeter (g/cm^3)
	Energy	
gallon per minute (gal/min)	0.06309	liter per second (L/s)
	Radioactivity	
picocurie per liter (pCi/L)	0.037	becquerel per liter (Bq/L)
	Weight	
ounce (oz.)	28.35	grams (g)

- Temperature in degrees Celsius (°C) may be converted to degrees Fahrenheit (°F) as follows:°F = (1.8×°C)+32
- Vertical coordinate information is referenced to the North American Vertical Datum of 1988 (NAVD 88).
- Horizontal coordinate information is referenced to the North American Datum of 1983 (NAD 83).
- Altitude, as used in this report, refers to distance above the vertical datum.
- Specific conductance is given in microsiemens per centimeter at 25 degrees Celsius (µS/cm at 25°C).
- Concentrations of chemical constituents in water are given either in milligrams per liter (mg/L) or micrograms per liter (µg/L).

EXPLANATION OF STRATIGRAPHIC, LITHOLOGIC, BEDDING, FRACTURE, AND GEOPHYSICAL LOG HEADINGS

Depth	Depth, in feet below land surface
Age	Geologic age
Form	Stratigraphic formation
Depth and Thickness	Depth in feet below land surface and thickness in feet of stratigraphic formations
Gamma	Gamma radiation log, in counts per second (CPS)
Litho	Generalized lithology overlying indicated log; light blue indicates sandstone, blue indicates sandstone with some siltstone and claystone, tan indicates claystone and siltstone, and black indicates carbonaceous zone
Neutron Porosity	Neutron porosity log, in fraction of total volume occupied by pores or voids (V/V)
Bulk Density	Bulk density log, in grams per cubic centimeter (g/cc)
ATV MN	Acoustic televiewer log oriented to Magnetic North
OTV MN	Optical televiewer log oriented to Magnetic North
Bedding TN	Tadpole plot of planar bedding features oriented to True Geographic North, body of tadpole indicates dip angle and tail indicates the direction of dip
Bedding Stereo TN	Lower-hemisphere, equal-area projection of poles for planar bedding features to True Geographic North
Sonic Amplitude	Color image of the sonic amplitude log, color darkens with higher return-signal strength, in millivolts (MV)
Sonic Arrival Time	Log of first arrival time of sonic signal, in micro-seconds (USEC)
Caliper Three Arm	Log of hole diameter measured by the three-armed caliper, in inches (Inch)
Caliper Single Arm	Log of hole diameter measured by the one-armed caliper, in inches (Inch)
Fracture Density	Number of fractures per 50 foot interval, blue indicates water bearing.
Fracture TN	Tadpole plot of planar fracture features oriented to True Geographic North, body of tadpole indicates dip angle and tail indicates the direction of dip, blue indicates water bearing
Fracture Stereo TN	Lower-hemisphere, equal-area projection of poles for fractures, in degrees
Breakout TN	Breakout feature oriented to True Geographic North
Fl Res	Log of fluid resistivity collected on date indicated by color [6/11 (gray), 6/18 (blue), 7/17 (green), 7/25 (purple), and 10/2/2012 (black)], in Ohm meters (Ohm-m)
Fl Res Sample	Fluid resistivity of specific-depth water samples collected on 6/19 and 7/25/2012, in Ohm meters (Ohm-m)
EMFlow	Flow measured by electromagnetic flowmeter log in stationary and trolling modes, in gallons per minute (Gal/min)
HPFlow	Flow measured by heatpulse flowmeter in stationary mode, in gallons per minute (Gal/min)
Temp	Log of temperature collected on date indicated by color as above, in degrees Celsius (Deg C)
Spec Cond	Log of specific conductance collected on date indicated by color as above, in microsiemens per centimeter at 25 degrees Celsius (μS/cm @ 25 Deg C)

Spec Cond Sample	Specific conductance of specific-depth water samples collected on 6/19 and 7/25/2012, in microsiemens per centimeter at 25 degrees Celsius (μS/cm @ 25 Deg C)
Density Porosity	Log of density porosity, in fraction of total volume occupied by pores or voids (V/V)
Induction Resistivity	Resistivity of the formation from induction log, in ohm meters (Ohm-m)
Rwa	Formation water resistivity estimated for selected sandstone intervals based on Archie's Equation in ohm-meters; porosity derived from log indicated in parentheses.

AUTHOR'S NOTE

The U.S. Geological Survey and the Bureau of Topographic and Geologic Survey used different reference numbers for the Gleason test hole location. The U.S. Geological Survey used test hole ID# BR-889 for all water-related bore hole tests and analyses. The Bureau of Topographic and Geologic Survey used core ID# BRA015-0204 for the core and rock analysis. Both numbers refer to the same location.

GEOHYDROLOGIC AND WATER-QUALITY CHARACTERIZATION OF A FRACTURED-BEDROCK TEST HOLE IN AN AREA OF MARCELLUS SHALE GAS DEVELOPMENT, BRADFORD COUNTY, PENNSYLVANIA

By Dennis W. Risser, John H. Williams, Kristen L. Hand, Rose-Anna Behr, and Antonette K. Markowski

ABSTRACT

The geohydrology and water quality of the Gleason test hole that penetrated fractured sedimentary rock in Bradford County, Pennsylvania was characterized through the integrated analysis of core, geophysical logs, and specific-depth water and gas isotope samples. The stratigraphy and lithology, fractures, water-bearing zones, groundwater quality, and isotopic signatures of hydrocarbons of the bedrock penetrated by the test hole were described. The investigation, completed in 2012 as a cooperative project between the Pennsylvania Department of Natural Resources, Bureau of Topographic and Geologic Survey and the U.S. Geological Survey, resulted in a detailed characterization of the fractured bedrock and its water-bearing zones, and provided an evaluation of the depth and composition of fresh and saline groundwater in an area of intensive development of natural gas from the Marcellus Formation.

The Gleason test hole was cored to a depth of 1,664 feet in an upland setting of high relief on Armenia Mountain. The test hole penetrated 98 feet of the Pottsville Formation of Pennsylvanian age, 584 feet of the Huntley Mountain Formation of Mississippian and Late Devonian age, and 982 feet of Catskill Formation of Late Devonian age. The Catskill Formation was distinguished from the Huntley Mountain Formation on the basis of more abundant and thicker packages of red and grayish-red interbedded sandstones, claystones, and siltstones. Carbonaceous layers and fragmented plant fossils were noted throughout the Huntley Mountain and Catskill Formations. The carbonaceous zones within the Catskill Formation correlated with significant spikes of elevated radioactivity on the natural gamma logs. Bedding features penetrated by the test hole were characterized as planar with noticeable crossbedding. Bedding was estimated to have a strike of 194 degrees and dip about 3 degrees to the northwest. Most of the fractures were parallel to bedding, with moderately to steeply dipping fractures present but less common. The frequency of fractures decreased with depth, with the upper 150 feet being most heavily fractured. Few fractures were penetrated below a depth of 800 feet. The orientation of breakouts discontinuously present in selected mudstone units between 785 to 1475 feet bls indicated that the direction of maximum horizontal stress is 070, which is consistent with regional estimates.

The depths of fresh and saline water-bearing zones were identified in the test hole by geophysical-log analysis and, for inflow zones, verified by specific-depth groundwater sampling by the use of a wire-line point sampler. Under ambient conditions, a total of about 7 gallons per minute of fresh groundwater entered the test hole from multiple fractures between 50 and 294 feet below land surface.

Because the composite-head water level was about 270 feet below land surface, much of the freshwater cascaded into the hole. The freshwater inflow, which had total dissolved solids concentration of 87 milligrams per liter, moved downward and exited the hole at fractures at 553, 661, and 712 feet below land surface. Although the salinity of water in the outflow zones could not be collected with the point sampler, the apparent substantial fracture transmissivity and low hydraulic head of those zones in contrast to the interval below suggested that they were freshwater bearing. Below the 712-foot zone, the temperature log approached the geothermal gradient, which indicated little ambient fluid flow and minimal fracture transmissivity below this depth. A petrophysical log analysis indicated that the formation water in sandstone intervals below 880 feet was highly saline. Saline-water inflows from fractures at 914 and 1,026 feet below land surface were identified on the video and specific conductance logs. The seepage from these zones was highly saline water with a minimum total dissolved solids concentration of 12,700 milligrams per liter.

Methane was measured from samples of water and core. The concentration of methane ranged from 7.8 to 37 milligrams per liter from three samples of saline water, and was 0.0003 milligrams per liter in one freshwater sample from 550 feet below land surface. The isotopic ratios of $^{13}C/^{12}C$ and $^{2}H/^{1}H$ of methane in the saline water indicated that these gases are likely of thermogenic origin. The isotopic ratios of methane extracted from a carbonaceous zone in the core at 1,310 feet below land surface also indicated a thermogenic origin.

A depth of active, fresh groundwater circulation of between 700 to 900 feet below land surface in the high-relief upland setting of the Gleason test hole is consistent with the deepest occurrence of fresh groundwater reported during gas-well drilling in bordering New York counties. The depth of active freshwater circulation was at an altitude below local streams near the Gleason test hole, but above the altitude of the main stem of Tioga River, which drains Armenia Mountain to the west, and the altitude of Alba Creek at Alba near the base of the steep topographic slope to the east.

INTRODUCTION

The analysis of core, geophysical logs, and specific-depth water-quality samples provides efficient means for the geohydrologic and water-quality characterization of fractured bedrock. The purpose of this study was to apply this integrated analysis in upper Devonian, Mississippian, and lower Pennsylvanian bedrock penetrated by a test hole in Bradford County, Pennsylvania in an area of intensive development of natural gas from the Marcellus Formation. The analysis provided a detailed stratigraphic profile of the Catskill Formation to aid the geologic mapping and an evaluation of the depth and composition of fresh and saline groundwater, which was not well documented in the area prior to the boom in shale-gas exploration.

The multi-disciplinary characterization of the test hole was done in 2012 as a cooperative project between the Pennsylvania Department of Natural Resources, Bureau of Topographic and Geologic Survey (BTGS) and the U.S. Geological Survey (USGS). The test hole was drilled on Tioga State Forest lands in western Bradford County as part of the STATEMAP bedrock mapping of the Troy 7.5-minute quadrangle (Behr and Hand, 2013). STATEMAP is a component of the National Cooperative Geologic Mapping Program (U.S. Geological Survey, 2013). This report describes the study site, test hole, and methods used. It presents an integrated analysis of the core, geophysical logs, water-quality, and gas-isotopic data to characterize the stratigraphy and lithology, fractures, water-bearing zones, groundwater quality, and isotopic signatures of hydrocarbons penetrated by the test hole.

Study Site and Test Hole

The BTGS contracted exploratory wire-line, diamond-core drilling in the headwaters of the Tioga River watershed in the Gleason 7.5 minute quadrangle, Bradford County, Pennsylvania (Figure 1). The site is in Tioga State Forest (District 16), Tract 588, about 4.5 miles northwest of Canton and 10 miles east-northeast of Blossburg. Coring of the test hole was completed on June 4, 2012. The test hole was open until it was decommissioned by filling with concrete grout on October 5, 2012.

The Gleason test hole was situated at 41.71188 degrees north latitude and 76.88832 degrees west longitude near the top of Armenia Mountain. It was located on the southern limb of the Blossburg Syncline, a regional broad open syncline with a gentle plunge to the southwest (Faill, 2011; McLaurin and Dodge, 2012; Behr and Hand, 2013). Altitude of land surface at the site is 2,365 feet. The hole was cored to a depth of 1,664 feet below land surface (bls) penetrating the Pottsville, Huntley Mountain, and Catskill formations.

The bottom of the Gleason test hole was at an altitude of 700 feet, about 520 feet below the altitude of any streams in the Tioga River headwaters shown in Figure 1. The water level in the test hole on June 18, 2012 was 270 feet bls (altitude 2,095 feet). The nearest local streams (Rundell and Rathbone Creeks) are at an altitude of about 2,000 feet. The altitude of the regional drainage, the main stem of the Tioga River downstream of Blossburg about 9.8 miles to the west, is 1,220 feet. Although the test hole penetrates much below the surface-water drainage, it is completed about 5,000 feet above the Marcellus Formation. In the nearest gas well about 1.7 miles to the northeast, the top of the Marcellus Formation is 7,100 feet bls at an altitude of about 4,900 feet (Pennsylvania Department of Environmental Protection, 2012).

Methods

The methods used to collect and analyze the core, geophysical logs, and specific-depth water and gas isotope samples are described in the following sections.

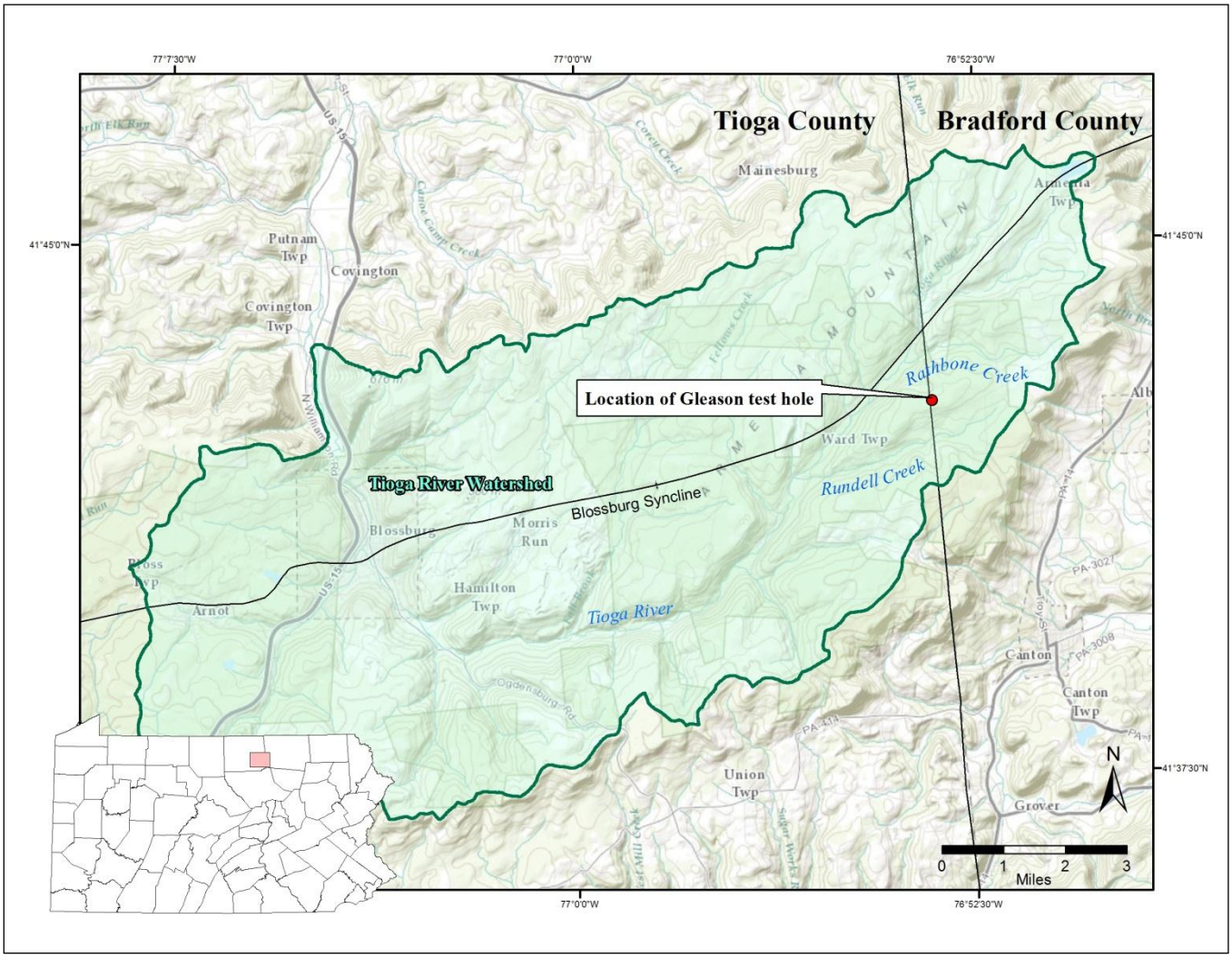

Figure 1. Location of the Gleason test hole in the Tioga River watershed of Tioga and Bradford Counties, Pennsylvania. The Blossburg Syncline is northwest of the test hole location and plunges to the southwest (Faill, 2011; McLaurin and Dodge, 2012; Behr and Hand, 2013). Inset map shows location within the state. Base map is ESRI Topographic base map.

Core

The test hole was cored with NX core barrel that provided a 2-inch diameter rock core and made a hole about 3.3 inches in diameter for its entire depth. Steel casing was set in the test hole to a depth of 9 feet bls. Immediately following the coring operation, the test hole was flushed by injecting water through the drill pipe into the bottom of the test hole at a rate of 32 gal/min for 2 hours, resulting in the total injection of 3,840 gallons, none of which returned to the surface. The injected water was obtained from nearby Rundell Creek. The water was injected so that the hole would be filled with clear water, which would facilitate the collection of high-resolution borehole images with the optical televiewer. The chemical composition of the injected water was not analyzed, but water withdrawn from the same stream for drilling operations several days earlier had a specific conductance of 28 µS/cm. Continuous core was collected from the test hole and is stored in the BTGS core library in Middletown, Pa. The core is available for examination upon request.

A detailed physical description of the core by BTGS recorded characteristics such as color,

lithology, grain size, relative carbonate content, fossil assemblages, minerals, carbonaceous zones, and other significant details. Measurements of the core were made to the tenth of a foot. A Munsell Rock-Color Chart was used for color standardization and the American Stratigraphic Company Grain size comparator for grain size. Detailed core descriptions are in Appendix 1.

Four sections of core were selected for methane isotope analysis. An isotopic analysis of natural gas is needed in order to better understand its origin, occurrence, maturity, and migration. Isotopic characterization of the methane provides a unique identification or signature, which is useful as supportive documentation for source determination. This signature helps identify the gas as naturally biogenic (microbial in origin), thermogenic, mixed, or indicates whether the gas composition is influenced by anthropogenic sources (Coleman and others, 1993). For this purpose, carbonaceous enriched zones in the Huntley Mountain and Catskill Formations of the test hole were targeted.

Core samples were prepared following a protocol provided by the analytical laboratory. The sample was cut with a hammer and chisel to a size weighing between 100 and 150 grams (3.5-5.3 oz.). The sample was tightly wrapped in aluminum foil and sealed in a cellophane sample bag. The seal was reinforced with clear packing tape. The sample was labeled with exact weight and identifying information and shipped overnight to the laboratory.

Geophysical Logs

Caliper, deviation, nuclear, electric, induction, sonic, image, and fluid logs were collected from the test hole. The nuclear logs were natural gamma, neutron, and gamma-gamma logs. Electric logs were self-potential, single-point resistance, and normal resistivity. Image logs were video, acoustic televiewer, and optical televiewer. Fluid logs were temperature, fluid resistivity, and flow. The geophysical logs and their dates of collection are presented in Table 1. The geophysical logs were collected by ARM Geophysics under contract with the BTGS and by USGS between June 11 and October 2, 2012 (Table 1). The geophysical logs were depth adjusted where needed to best match the depths associated with the acoustic televiewer log, which was used as the standard. An additional depth adjustment was needed to best match the video log due to cable stretch. The true depth of the video logs was estimated by multiplying the displayed depth by 1.0066 and subtracting 1.6 ft. The distribution and orientation of bedding was determined through analysis of the optical televiewer log by ARM Geophysics. The distribution and orientation of fractures determined through analysis of the optical televiewer log by ARM Geophysics was slightly modified by the USGS based on an integrated analysis of the optical and acoustic televiewer and video logs. The geophysical logs collected for this study are available for download in Log Ascii Standard (LAS) and Portable Document Format (PDF) formats from Appendix 3.

The geophysical logs are briefly summarized below. Additional information on these types of geophysical logs is presented in Kelley (1969), Keys (1990), and Rider and Kennedy (2011).

Caliper logs record hole diameter and are collected with a probe equipped with one or three spring-loaded arms. Changes in test hole diameter may be correlated to drilling and construction procedures, competency of lithologic units, and fractures. Stationary flowmeter measurements were collected in competent intervals above and below potential fracture zones as identified on the caliper and optical and acoustic televiewer logs.

Deviation logs measure the vertical deviation and spatial trajectory of the test hole. Deviation was measured with two inclinometers and a three-component magnetometer included

with the acoustic televiewer. The deviation logs were used to determine the spatial trajectory of the test hole and correct the apparent orientation of structural features identified on the acoustic and optical televiewer logs to their true orientation.

Natural gamma logs measure the amount of natural gamma-ray radiation emitted by the formation surrounding the test hole. Clay-bearing rocks commonly emit relatively high gamma radiation because they include weathering products of potassium feldspar and mica and tend to concentrate uranium and thorium by ion absorption and exchange. Naturally occurring sources of gamma radiation include potassium-40 and daughter products of the uranium- and thorium-decay series. The vertical resolution of the gamma tool is 1 to 2 feet. The gamma log was used in the delineation of lithology, specifically identification of sandstone, claystone, and carbonaceous zones.

Neutron logs measure the number of neutrons received at a detector from a neutron source in the probe after the neutrons have interacted with the formation surrounding the test hole. The majority of the neutron interactions are in response to the amount of hydrogen present, which is largely a function of the water content. Total formation porosity was estimated from the neutron log. Neutron logs commonly correlate with gamma logs because zones with high estimated porosities (low neutron count rates) are commonly associated with clay-bound water.

Gamma-gamma logs measures the bulk density of the formation surrounding the test hole based on the attenuation of radiation

Table 1. Types of geophysical logs and dates of collection from the Gleason test hole, Bradford County, Pennsylvania.

LOGS COLLECTED	Agency or Company Collecting the Geophysical Logs and Date Collected					
	ARM	USGS	USGS	USGS	USGS	USGS
	6/11-12/2012	6/18-19/2012	7/16/2012	7/17/2012	7/25/2012	10/2/2012
Single-arm caliper	X					
Three-arm caliper		X				
Natural gamma	X	X	X			
Neutron	X					
Gamma-gamma	X					
Spontaneous potential	X					
Single-point resistance	X					
Normal resistivity	X					
Induction conductivity		X				
Full waveform sonic		X				
Video				X (1000 ft)	X (1000 ft)	X
Acoustic televiewer		X				
Optical televiewer	X					
Temperature	X	X	X		X	X
Fluid resistivity	X	X	X		X	X
Flow		X				

[ARM, ARM Geophysics; USGS, U.S. Geological Survey; X(1000 feet), indicates the video log was collected to the depth indicated in feet below land surface. If depth not noted, video was collected for entire depth of hole].

emitted from a gamma source and received at two detectors. The gamma-gamma log was converted to quantitative estimates of density and porosity.

Spontaneous-potential logs (sometimes referred to as SP or self-potential) measure the electrical potentials that develop in the test hole at lithologic and water-quality interfaces. Spontaneous potential is largely a function of chemical reactions that occur within the test hole fluids and the type and quantity of clay present. Electrochemical effects tend to result from the migration of ions from more concentrated to less concentrated fluids.

Single-point resistance logs measure the electrical resistance from points within the test hole to an electrical ground at land surface. In general, resistance increases with increasing grain size and decreases with increasing test-hole diameter, fracture density, and dissolved-solids concentration of the water. Single-resistance logs are affected by the dissolved-solids content of the test hole fluid. The single-point resistance log was used in the delineation of lithology and fracture zones.

Normal-resistivity logs measure the electrical resistivity of the rocks and water surrounding the test hole. Electrical resistivity measurements consist of short-normal (16 inches) and long-normal (64 inches) resistivities, or near and far resistivities, respectively, that have two different volumes of investigation. Electrical resistivity measurements are affected by the clay content and porosity of the rocks and by the dissolved-solids concentration of the pore fluid. The normal-resistivity logs are most effective in formations having high electrical resistivities (low conductivities).

Induction-conductivity logs measure the electrical conductivity of rocks and water surrounding the test hole. The induction tool, which is operated at a frequency of 40 kilohertz (kHz), has a focused radius of investigation and a vertical resolution of about 2 feet. The tool response generally is not affected by the electrical properties of the test hole fluid for diameters less than 8 inches. Electrical conductivity measurements are affected by the clay content and porosity of the rocks and by the dissolved-solids concentration of the pore fluid. Induction-conductivity logs are most effective in formations having high electrical conductivities (low resistivities). The induction-conductivity log was converted to an induction-resistivity log and used along with the gamma and neutron and gamma-gamma porosity logs to estimate fluid resistivity of the pore fluid in selected sandstone intervals through application of Archie's Equation (Archie, 1942).

Full-waveform sonic logs measure the amplitude and travel time of acoustic waves transmitted through rocks and water surrounding the borehole. The sonic tool is equipped with a single transmitter operated at a frequency of 24 kHz and dual receivers spaced approximately 2 and 3 feet from the transmitter. Compressional wave slowness, in units of microseconds per foot (the inverse of velocity) was estimated from the acoustic travel times. Slowness is affected primarily by rock elastic properties and commonly correlates with density. Slowness also increases substantially where rocks are highly fractured.

Video logs record images of the test hole collected with a submersible color camera. Video logging techniques and equipment are described by Johnson (1996). Down-looking fisheye views of the test hole and side-looking views of the test hole wall were recorded. The video logs were used to identify lithology, bedding and fractures, breakouts, test hole-wall staining, and water flow including cascading water above the water level, particle movement below the water level, shimmering fluid indicating saline water, and bacterial growth.

Acoustic-televiewer logs record a 360-degree magnetically oriented acoustic image of the test hole wall (Williams and Johnson, 2004).

Acoustic-televiewer logs can be collected in clear or turbid water. Structural features with widths greater than 0.02 ft can be identified. The acoustic-televiewer log provided high-resolution information on test hole-wall roughness and the distribution and orientation of fractures, and breakouts

Optical-televiewer logs record a 360-degree oriented optical image of the test hole wall (Williams and Johnson, 2004). The OTV logs can be collected above the water level, and below water where the water is clear. Features with widths greater than 0.008 feet can be identified. The optical-televiewer log was used to characterize the distribution and orientation of bedding, fractures, and breakouts as well as lithologic contacts and test hole-wall staining. The apparent dips of bedding planes and fractures were corrected to true dip angles based on the deviation and caliper logs; dip directions were adjusted from magnetic north to true north based on the local magnetic declination of 11.5 degrees west of true north.

Temperature logs measure the temperature of the air and water in the test hole. Repeated temperature logs were collected from the test hole under ambient conditions. Although part of the standard procedure, temperature logs were not collected under pumped conditions from the test hole. Because of limitations related to the small diameter of the test hole and great depth of water level, a submersible pump was not available that would significantly impact the large downward flow that occurred in the test hole, and therefore, logging under pumped conditions was determined not to be worthwhile. In the setting of the test hole, temperature gradients less than the geothermal gradient in the surrounding rocks indicate intervals with vertical test-hole fluid flow. As test-hole fluid flow decreases, the temperature gradient of water in the test hole approaches the geothermal gradient. Downflow is characterized by test-hole water cooler than that in equilibrium with the geothermal gradient. Conversely, upflow is characterized by test hole water warmer than that in equilibrium with the geothermal gradient. Williams and Eckhardt (1987) estimated a geothermal gradient of about 1°F (0.56°C) per 100 feet based on temperature logs from 26 deep bedrock wells in east-central Pennsylvania. Temperature logs were used with the fluid-resistivity, specific conductance, and flow logs to identify water-bearing zones and intervals of flow under ambient conditions.

Fluid-resistivity logs measure the electrical resistivity of the water in the test hole. The electrical resistivity of the water is related to its dissolved-solids concentration. Repeated fluid-resistivity logs were collected under ambient conditions. Although part of the standard procedure, fluid-resistivity logs were not collected under pumped conditions from the test hole for the reason presented above. Specific conductance logs were calculated from the fluid resistivity and the temperature logs. Fluid-resistivity and specific conductance logs were used with the temperature and flow logs to identify fresh and saline water-bearing zones.

Flow logs record the direction and rate of vertical fluid flow in the test hole. Flow logs were collected from the test hole under ambient conditions. Although part of the standard procedure, flow logs were not collected under pumped conditions from the test hole for the reason presented above. Heat-pulse and electromagnetic flowmeters were used to measure vertical flow. The heat-pulse flow meter measures the travel time of a thermal pulse between a set of upper and lower thermistors (Hess, 1982). The heat-pulse flowmeter, which was used in a stationary mode with a flexible rubber diverter fitted to the nominal diameter of the test hole, has a measurement range of 0.01 to 1.5 gal/min. An electromagnetic flowmeter was used to measure the higher flows encountered in the test hole. The electromagnetic flowmeter (Young and Pearson, 1995) measures fluid velocity based on

Faraday's Law, which states that the flow of an electrically conductive fluid through an induced magnetic field generates a voltage gradient that is proportional to its velocity. The electromagnetic flowmeter, which was used in stationary and trolling modes with a flexible rubber diverter, has a measurement range of 0.05 to 15 gal/min. The flow logs were used with the temperature and fluid-resistivity logs to identify flow zones and the direction and rate of flow between zones under ambient conditions.

Water-Quality Samples

Field and laboratory analysis of water samples provided estimates of the quality of water in the test hole at specific depths. The selection of sample depths was determined by analysis of the geophysical logs, especially the video, flowmeter, temperature, fluid resistivity, and specific-conductance logs. Depths were selected so that the water sampled was indicative, to the extent possible, of the water quality from a particular water-bearing zone or of one or more identified flow zones (Williams and Conger, 1990). However, because the individual water-bearing zones were not isolated (with multiple monitoring wells or packers) and sampled individually, the specific-depth sampling may represent mixtures of water from different intervals and should be viewed as a reconnaissance of water quality in the aquifer.

Water samples were collected under ambient (non-pumping) conditions at selected depths by the use of a stainless-steel point sampler. The sampler used in this study is remotely controlled by a wireline that operates a motor, which opens and closes a valve on the intake port of the sampler, allowing as much as one liter of water to be collected from the test hole at a selected depth. When the sampler was positioned at the selected depth, the valve was opened for about 5 minutes while the sampler filled with water, then the valve was closed and the sampler was raised to the surface. A round-trip to collect one liter of water from a depth of 1,000 feet required about one hour. About four liters of water from each selected depth interval were needed to obtain enough water for laboratory analysis of the selected analytes.

After retrieving the point sampler at the surface, water was transferred into the appropriate sampling containers; processed according to protocols outlined in Wilde and others (2004); preserved with acid and chilled (as required); and shipped to the laboratory by overnight express. Transfer of unfiltered samples was accomplished by opening the discharge port and allowing water to drain from the sampler into bottles. For samples requiring filtration, a 6-inch length of Teflon-lined tubing and a capsule filter with 0.45-micron size pores was attached to the discharge port of the point sampler. A cylinder of ultra-pure nitrogen gas was attached to the intake port of the point sampler, and nitrogen gas was used to push sample water through the capsule filter, which eliminated the need to open the sampler to the atmosphere. Samples for gases and stable isotopes were collected by draining water from the point sampler directly into a gas-sample "Isobag" without opening the sample intake port to the atmosphere. After filling all the required bottles for a sample from a specific depth, the stainless-steel point sampler was washed in the field with a 5% Liquinox soap solution and rinsed multiple times with tap water and deionized water.

Water samples were collected from five depths during June 19-20 and July 25-26, 2012 (Table 2). Samples were collected for analysis of field parameters, major ions, trace metals, radiochemicals, dissolved gases, and isotopic composition during June 19-20, 2012. Subsequently, a video survey was done in the test hole that showed the inflow of a white, milky looking substance at 914 feet bls. Because the fluid-resistivity logs indicated upward flow at that depth, additional samples were collected at 910 feet bls (above the inflow) during July 25-26, 2012, and were analyzed for nutrients, organic carbon, surfactants, strontium isotopes, volatile and semivolatile organic

compounds, diesel and gasoline-range organics, and glycols. Analytical results from all samples are in Appendix 2 and are available from the USGS National Water Information System database at http://waterdata.usgs.gov/nwis/inventory?agency_code=USGS&site_no=414243076531801.

The pH, water temperature, specific conductance, dissolved oxygen, oxidation-reduction potential, and turbidity were measured in the field with a multi-parameter meter. Field properties were measured as soon as possible after water was transferred out of the point sampler, but the water samples warmed, degassing was noted, and the values for temperature, dissolved oxygen, and oxidation-reduction potential drifted. Thus, these field values are probably not representative of the water at depth. Alkalinity was determined by titration to an inflection-point determined from titration in the field.

Samples for analysis of major ions, nutrients, and trace metals were sent to the USGS National Water Quality Laboratory (NWQL) in Denver, Colorado. Samples for radiochemical analysis were sent to Eberline Services Inc., a private laboratory under

Table 2. Depth-dependent water-quality samples collected and constituents analyzed in groundwater from the Gleason test hole, Bradford County, Pennsylvania.
[Type: U, unfiltered; F, filtered; Blank, field blank; bls, below land surface; N/A, not applicable; X, sample collected for analysis of the indicated chemical constituent; --, not sampled; VOC, volatile organic compound; SVOC, semivolatile organic compound]

Sampling dates	June 19-20, 2012					July 25-26, 2012	
Depth, in feet below land surface	550	915	1022	1500	Field Blank	910	Field Blank
Formation name	Huntley Mountain	Catskill	Catskill	Catskill	N/A	Catskill	N/A
Field parameters	X	X	X	X		X	
Major ions	X	X	X	X	X	X	X
Trace metals	X	X	X	X	X	X	X
Radiochemicals	X	X	X	X	X		
Dissolved gases and isotopes	X	X	X	X	X	X	
Nutrients						X	X
Organic carbon						X	X
Surfactants						X	X
VOCs & SVOCs						X	X
Gasoline range organics						X	X
Diesel range organics						X	X
Glycols						X	

contract to the NWQL. Samples for analysis of dissolved gases and stable isotopes were sent to Isotech Laboratories, Inc., and strontium isotopes were analyzed at the USGS Crustal Geophysics and Geochemistry Science Center in Denver, Colorado.

In addition to the five samples of water from the Gleason test hole, two field blanks were collected to evaluate contamination from field equipment and sampling procedures. The field blanks were prepared by pouring reagent-grade inorganic or organic-free water into the stainless-steel point sampler, then transferring the water into the appropriate sample containers in exactly the same procedure described above for the specific-depth environmental samples.

GEOHYDROLOGIC AND WATER-QUALITY CHARACTERIZATION OF THE GLEASON TEST HOLE

The geohydrology and water quality of the Gleason test hole was characterized through the integrated analysis of core, geophysical logs, and water-quality samples. The stratigraphy and lithology, fractures, water-bearing zones, groundwater quality, and isotopic signatures of hydrocarbons of the bedrock penetrated by the test hole are presented.

Spatial Trajectory of the Test Hole

Rotary holes drilled in dipping sedimentary bedrock tend to deviate at an angle perpendicular to bedding (Brown and others, 1981), and such was the case for the Gleason test hole. As determined from the deviation log, the test hole deviated 16.2 ft at an azimuth of 120 degrees at its total depth (Figure 2). The angle of the test hole from vertical generally increased with depth ranging up to 1.5 degrees near its bottom.

Stratigraphy and Lithology

The stratigraphy and lithology penetrated by the test hole were characterized through the analysis of the core. The natural gamma, neutron, density, image, and other geophysical logs provided supporting information in this analysis. The test hole penetrated Pennsylvanian, Mississippian, and Devonian clastic sedimentary bedrock of, in descending order, the Pottsville, Huntley Mountain, and Catskill Formations (Figure 3). Based on the information collected from the core, Pottsville Formation bedrock was penetrated at 2 feet bls and continued for 96 feet. The Pottsville primarily consisted of fine- to medium-grained sandstone with minor thin claystone interbeds. Six clay zones ranging from 0.25 to 0.5 feet in thick were penetrated. The dominant color of the formation was pale orange to yellowish gray with iron staining commonly present along bedding planes.

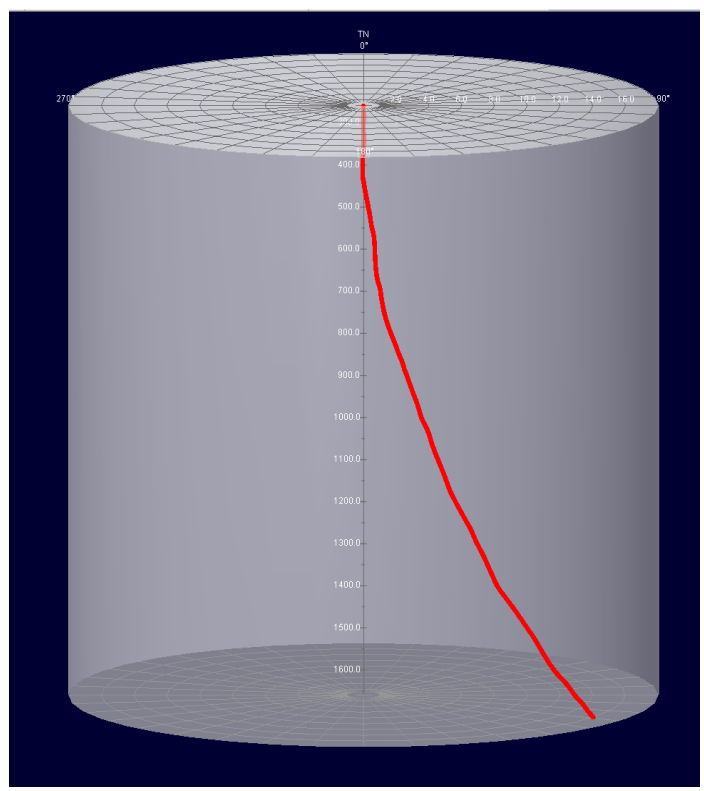

Figure 2. The angle of the test hole from vertical generally increased with depth ranging up to 1.5 degrees near its bottom.

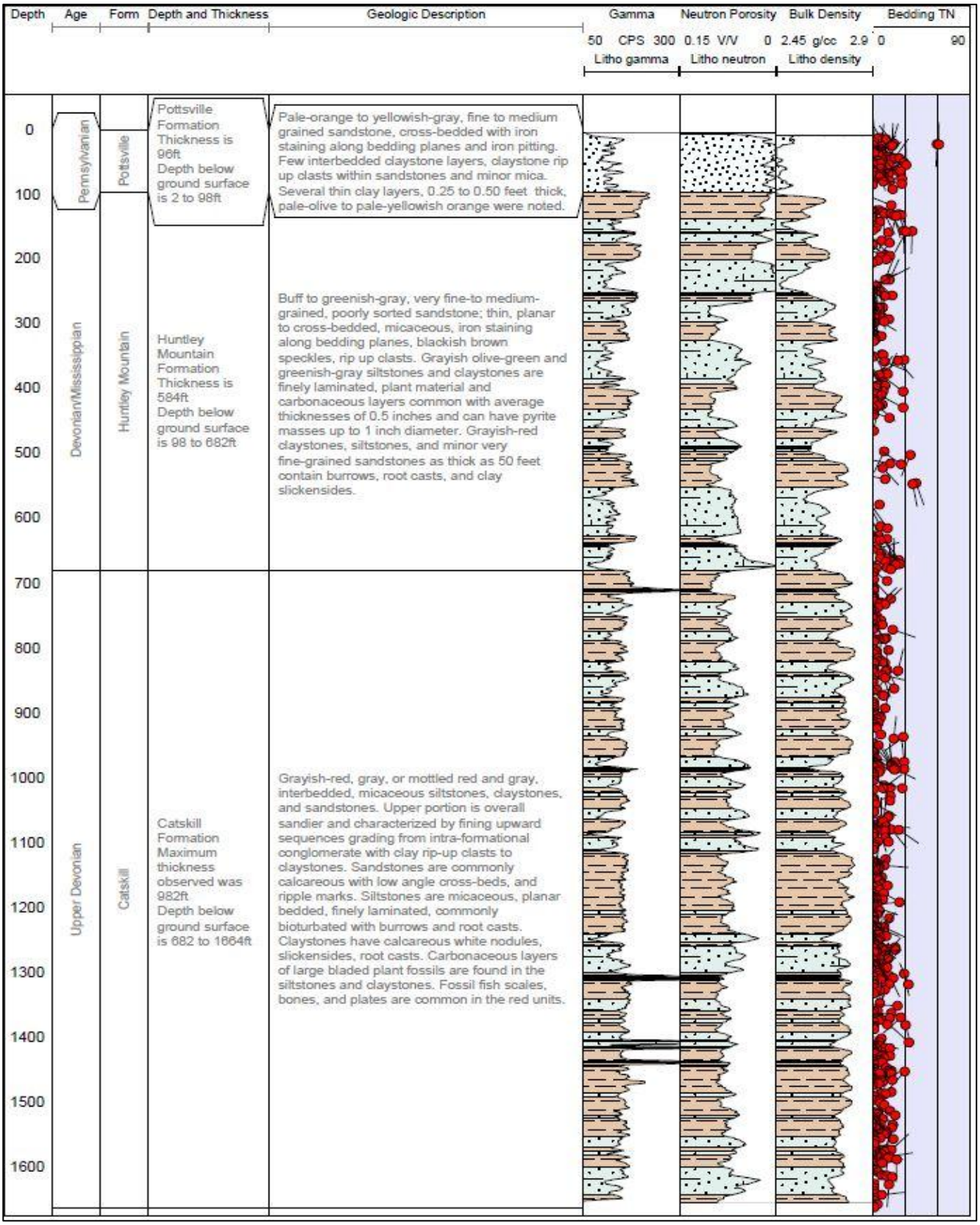

Figure 3. Logs of stratigraphy, lithology, natural gamma, neutron porosity, density, and bedding orientation for the Gleason test hole, Bradford County, Pennsylvania. (Explanation of log headings, units, and symbols are presented on page 7).

The Huntley Mountain Formation was penetrated from about 98 to 682 feet bls and is 584 feet thick. The Huntley Mountain was distinguished from the overlying Pottsville Formation on the basis of a change from predominantly sandstone to siltstone and claystone The Huntley Mountain consisted of buff to greenish gray, poorly sorted sandstones with cross-bedding and interbedded finely laminated claystones and siltstones. The claystones and siltstones ranged in color from grayish-olive green to greenish gray. Grayish-red claystone units with minor sandstone and siltstone were not uncommon and ranged in thickness from 14 to 50 feet. A fossil Devonian decapod (Figure 4) was present in the core at a depth of 502.2 feet bls.

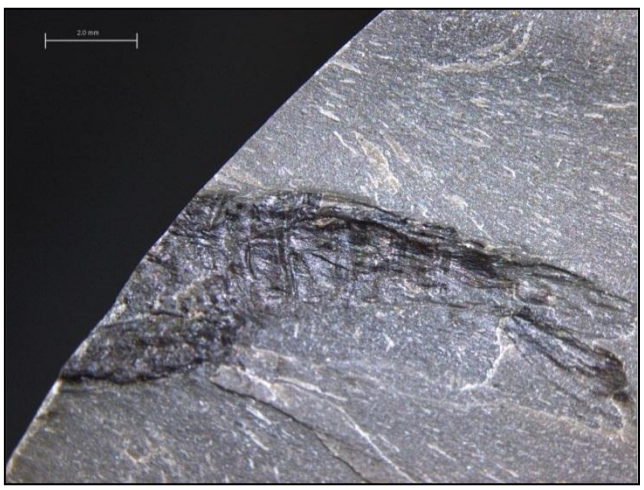

Figure 4. Devonian decapod, species currently unknown and under scientific review, present at a depth of 502.2 feet bls in the core from the Gleason test hole, Bradford County, Pennsylvania; specimen currently located in the Carnegie Museum collection.

The Catskill Formation was penetrated from about 682 feet bls to the total depth of the test hole at 1,664 feet bls. The Catskill was distinguishable from the Huntley Mountain Formation based on more abundant and thicker packages of red and grayish-red interbedded sandstones, claystones, and siltstones. The greater fine-grained content of the Catskill as compared to that of the Huntley Mountain Formation was further supported by the gamma and neutron logs, change in amplitude of the sonic log (Figure 3). Additionally, the gray sandstones of the Catskill are medium to light gray instead of greenish gray as those of the Huntley Mountain. The upper part of the Catskill Formation was dominated by fining-upward sequences, whereas the middle part of the formation is primarily interbedded grayish-red sandstones and siltstones. Fossil fish bones and plates were common in the red units.

Carbonaceous layers and fragmented plant fossils were present throughout the Huntley

Figure 5. Core sample of the carbonaceous layer seen within the Huntley Mountain Formation at 255 feet bls and sent for gas isotope analysis, Gleason test hole, Bradford County, Pennsylvania.

Mountain and Catskill Formations (Figures 3 and 5). The carbonaceous zones within the Catskill Formation at 713, 1310, 1408, 1417, and 1438 feet bls correlated with spikes of highly elevated radioactivity on the natural gamma logs, as shown for the entire test hole in figure 3 and for 1310 feet bls in Figure 6. Four samples from the carbonaceous zones, two from the Huntley Mountain and two from the Catskill, were collected for gas isotope analysis and are discussed later in the Gases and Stable Isotopes section of this report. Detailed strip logs and core descriptions are in Appendix 1.

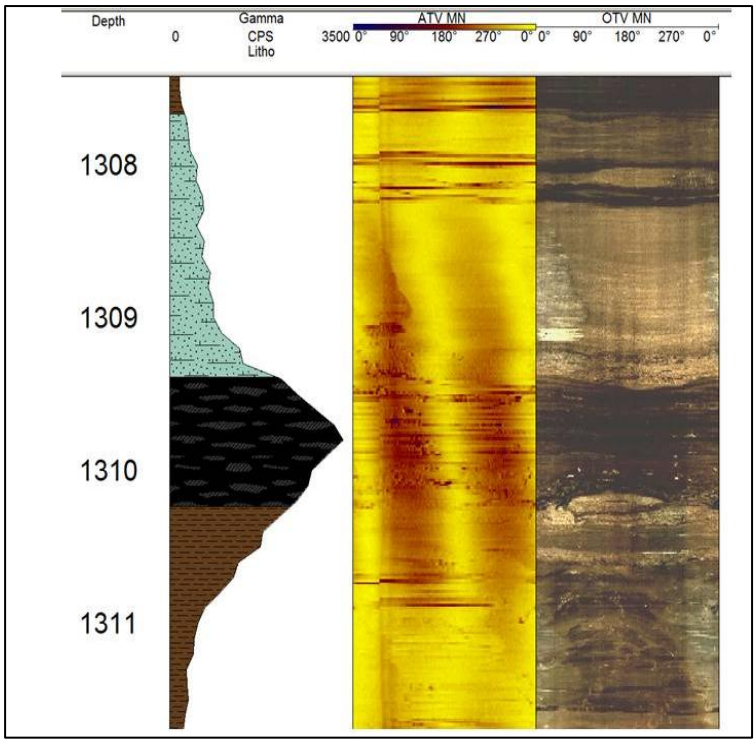

Figure 6. Gamma and lithologic logs and acoustic and optical televiewer images of carbonaceous zone penetrated at 1310 feet bls by the Gleason test hole, Bradford County, Pennsylvania (explanation of log headings, units, and symbols are presented on page 7).

Bedding

The character, distribution, and orientation of bedding features were determined from the analysis of the core and OTV log. Bedding features penetrated by the test hole were planar with noticeable crossbedding. The mean strike of beds was 194 degrees with a mean dip of bedding about 3 degrees northwest (Figure 7). Although displaying scatter due to the low bedding angle and abundant crossbedding, the mean bedding orientation was consistent with the position of the test hole on the southern limb of the Blossburg Syncline.

Fractures

The distribution and orientation of fractures penetrated by the test hole were characterized through the analysis of the core along with the acoustic and optical televiewer, video, caliper, and sonic logs (Figure 8). The frequency of fractures penetrated by the test hole decreased with depth (Figures 8 and 9). About 32 fractures were penetrated every 50 feet in the upper 150 feet of the test hole, which spanned the Pottsville and uppermost Huntley Mountain Formations. About six fractures were penetrated every 50 feet in the interval between 150 and 800 feet bls, which spanned the Huntley Mountain and upper Catskill Formations. Few fractures were penetrated below 800 feet bls. Fractures were very frequent at depths of about 100, 150, 250, 295, and 710 feet bls, as indicated by the nearly horizontal segments of the cumulative-frequency curve shown in Figure 9. The zones of increased fracturing generally displayed decreased waveform amplitudes on the sonic log. Most (about three-quarters) of the fractures were characterized as bedding-parallel fractures (Figure 10). The few steeply dipping fractures shown in Figure 10 matched the regional primary and secondary

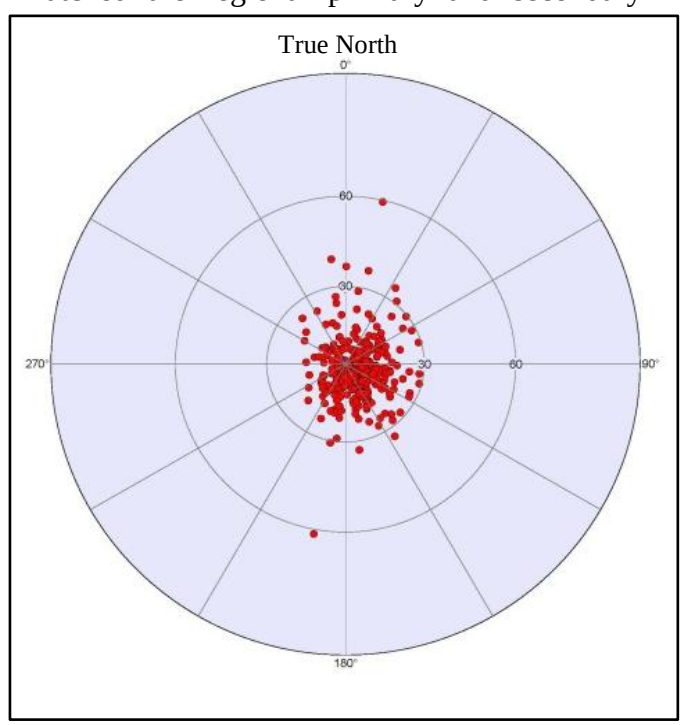

Figure 7. Lower-hemisphere, equal-area projection of poles for bedding orientations penetrated by the Gleason test hole, Bradford County, Pennsylvania.

joint sets with strikes of 150 and 070, respectively (Behr and Hand, 2013); though in the test hole, the primary joint set is less apparent than the secondary joint set, which was encountered more frequently in this location.

Breakouts, which are formed by spalling of bedrock fragments from the borehole wall parallel to the direction of minimum horizontal stress, were discontinuously present in selected mudstone units between 785 to 1475 ft bls (Figure 8). The orientation of the breakouts indicated that the direction of maximum horizontal stress is 070, which is consistent with regional estimates presented by Zoback and Zoback (1980).

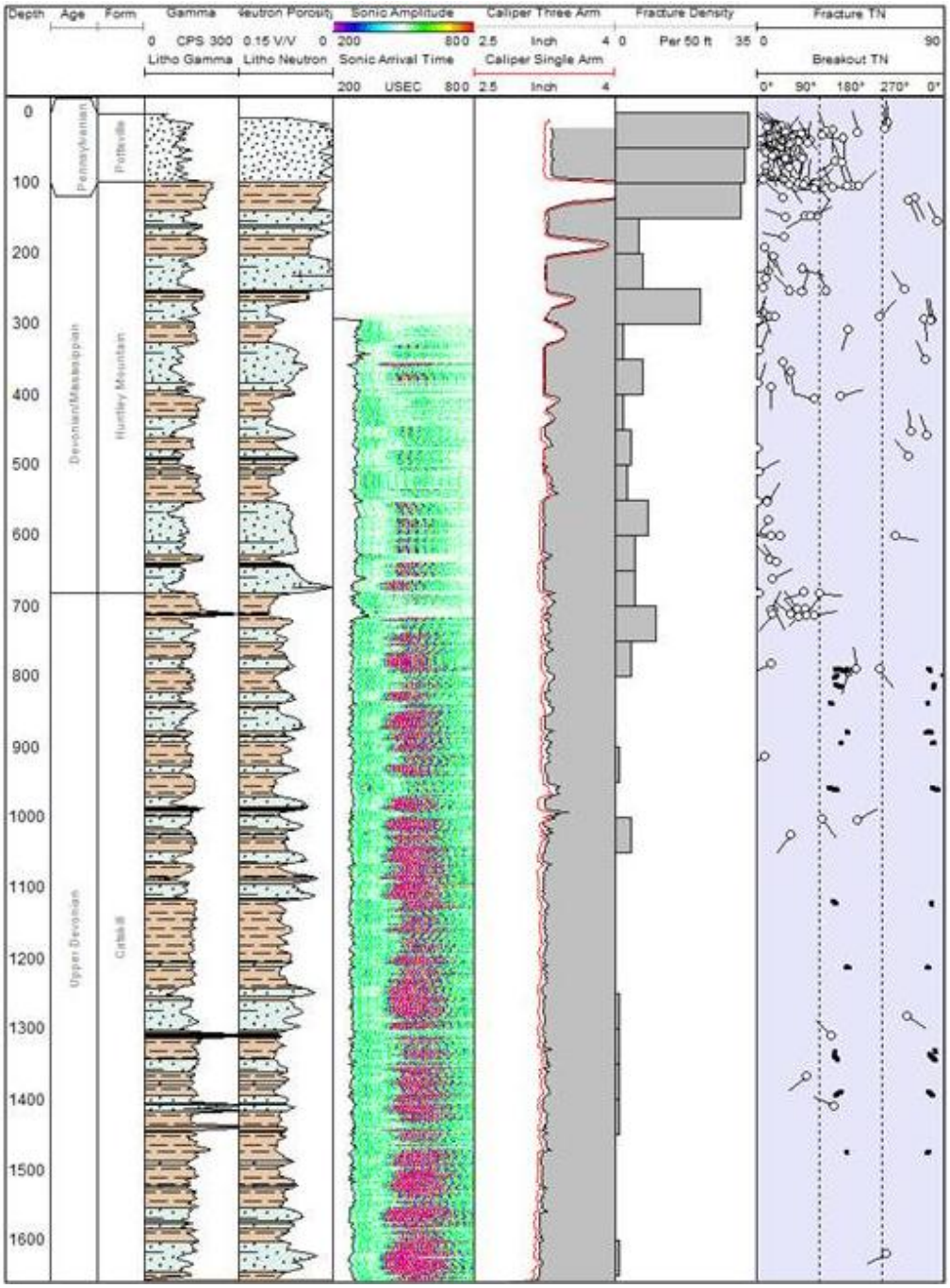

Figure 8. Stratigraphy, lithology with natural gamma and neutron, sonic amplitude and travel time, and caliper logs and of breakout and fracture orientation for the Gleason test hole, Bradford County, Pennsylvania (explanation of log headings, units, and symbols are presented on page 7).

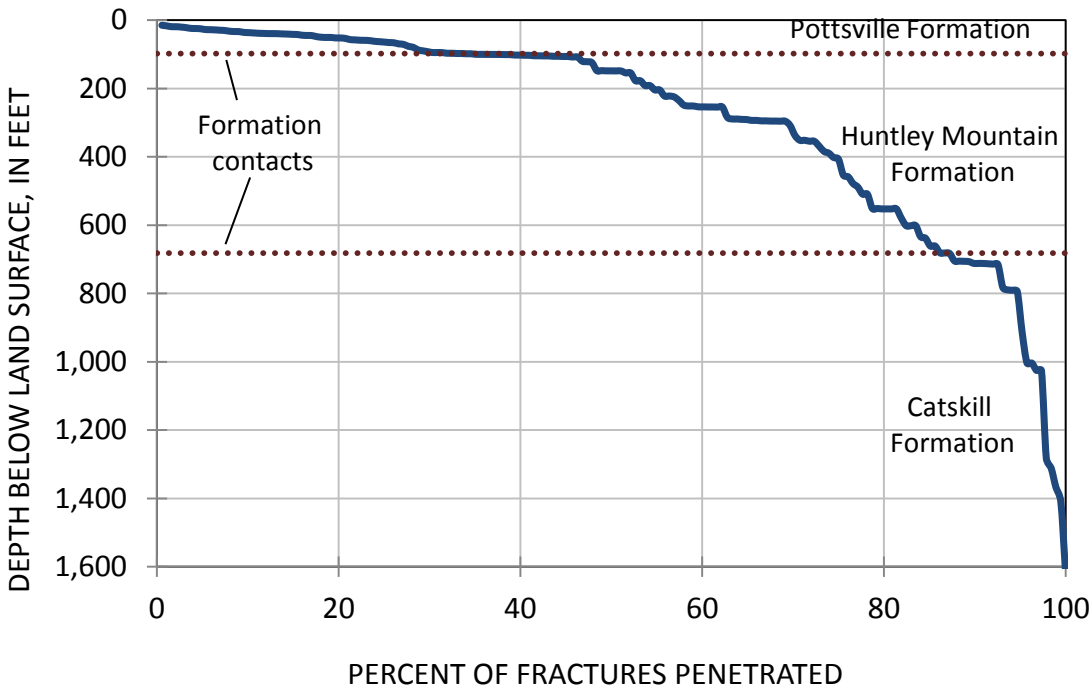

Figure 9. Cumulative frequency of penetrated fractures in relation to depth below land surface in the Gleason test hole, Bradford County, Pennsylvania.

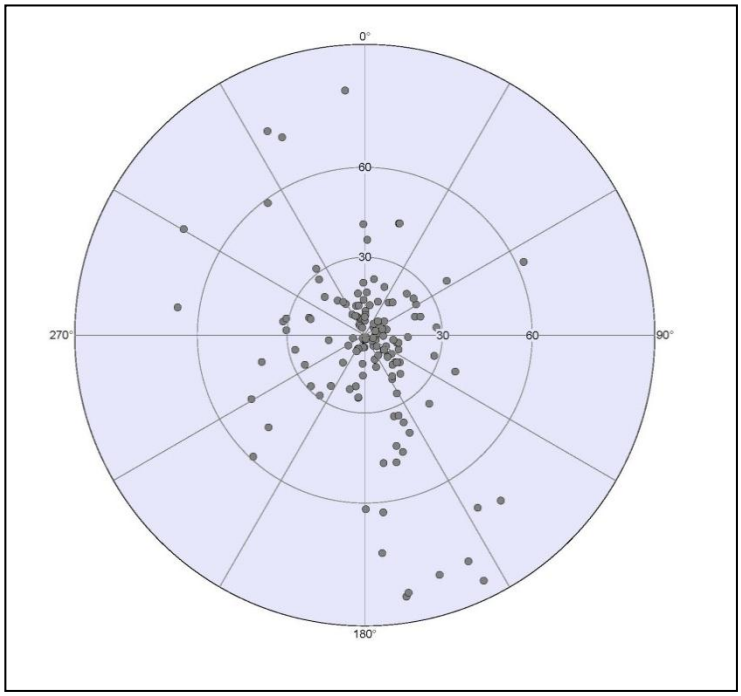

Figure 10. Lower-hemisphere, equal-area projection of poles for fractures penetrated by the Gleason test hole, Bradford County, Pennsylvania.

WATER-BEARING ZONES

The water-bearing zones penetrated by the test hole were characterized through the analysis of the temperature, fluid resistivity, specific conductance, and flow logs in conjunction with the stratigraphic, lithologic, and fracture characterization presented in the previous sections (Figure 11). Fluid temperature, fluid resistivity, and the derived specific-conductance logs were collected on six occasions between June 11 and October 2, 2012 to help document changes in water quality.

The test hole penetrated multiple water-bearing zones with differing hydraulic heads and with a wide range of transmissivity. The ambient composite water level in the test hole, which was largely controlled by the most transmissive water-bearing zones, was about 270 feet bls.

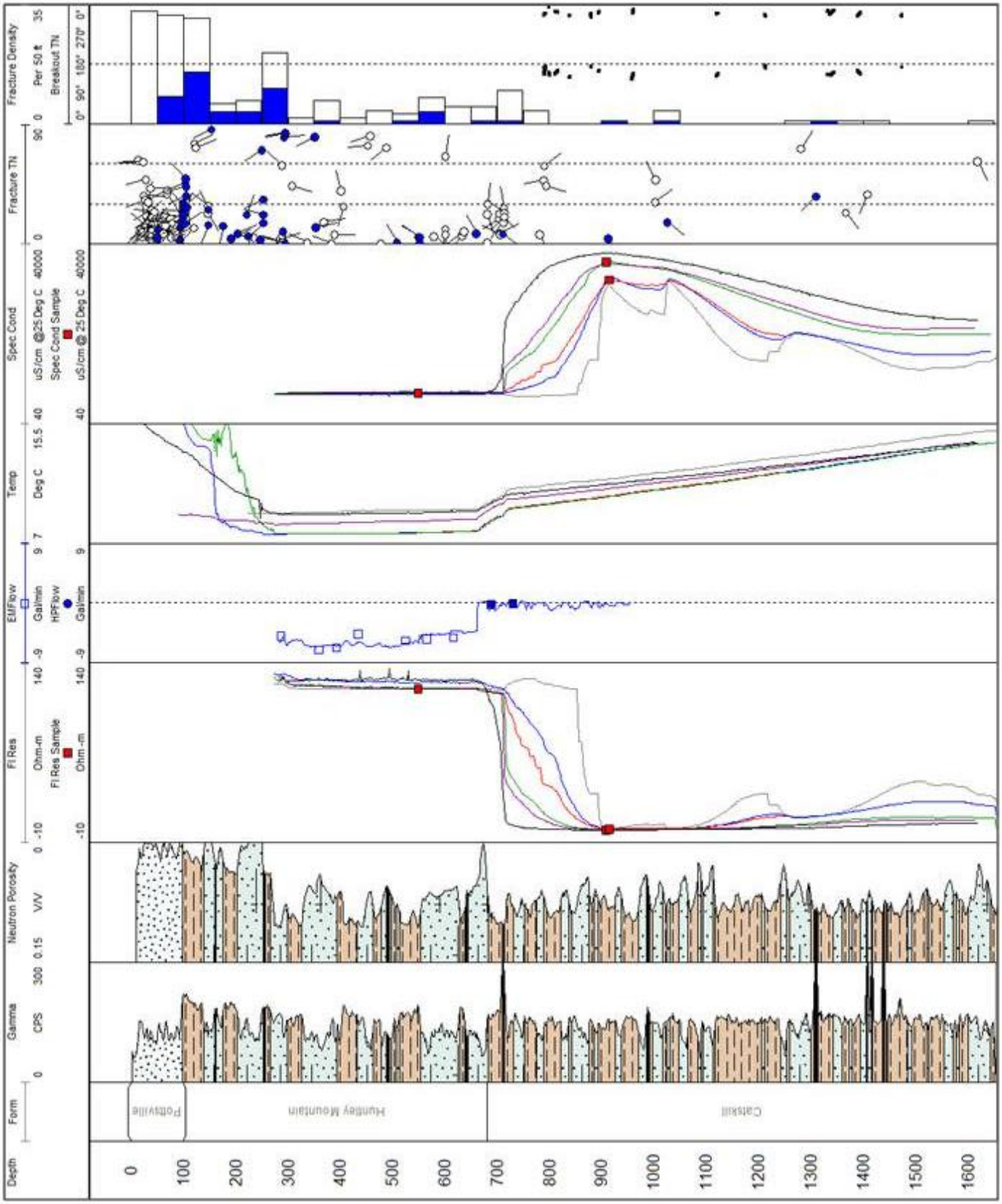

Figure 11. Logs showing stratigraphy, lithology, fluid resistivity, flow, temperature, fluid specific conductance, breakout orientation, and water-bearing fracture orientation and density for the Gleason test hole, Bradford County, Pennsylvania (explanation of log headings, units, and symbols are presented on page 7).

Above the composite water level in the well, water-bearing zones at 50 to 52, 96 to 106, 148 to 154, 192, 225, and 249 feet bls produced inflows of low specific-conductance water that cascaded down the test hole. The inflow zones consisted of subhorizontal, moderately dipping, and/or steeply dipping fractures (Figure 12).

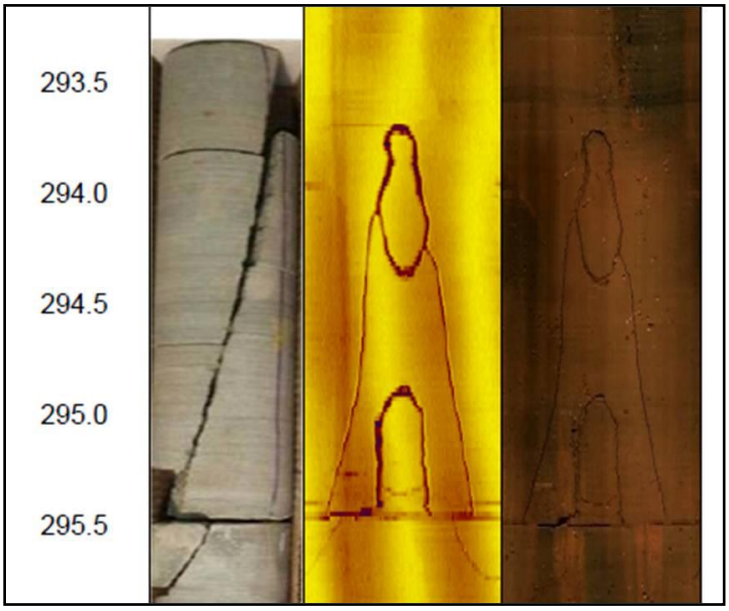

Figure 12. Core photograph and acoustic and optical televiewer images of three steeply dipping fractures and a subhorizontal fracture penetrated at about 294 feet below land surface by the Gleason test hole, Bradford County, Pennsylvania.

The cumulative downward flow of freshwater from these zones was about 5 gal/min, as measured on the flow log just below the composite water level (Figure 11). Inflows at the 225 and 249 feet zones jetted out of the bedrock under significant pressure from several points along the plane of the fractures (Figure 13). Temperature gradients measured in the test hole above the composite water level were variable due to the effects of the cascading water on the logging tool sensor.

Below the composite water level, a freshwater-bearing zone at 294 feet bls with a hydraulic head higher than the composite water level produced about 2 gal/min of additional downflow (Figure 11). The 294-foot inflow zone consists of three steeply dipping fractures and a subhorizontal fracture within the lower part of a 5-foot thick sandstone bed (Figure 12). The specific conductance of the water from this zone was just slightly higher than that of the cascading water from above. Inflow at this zone

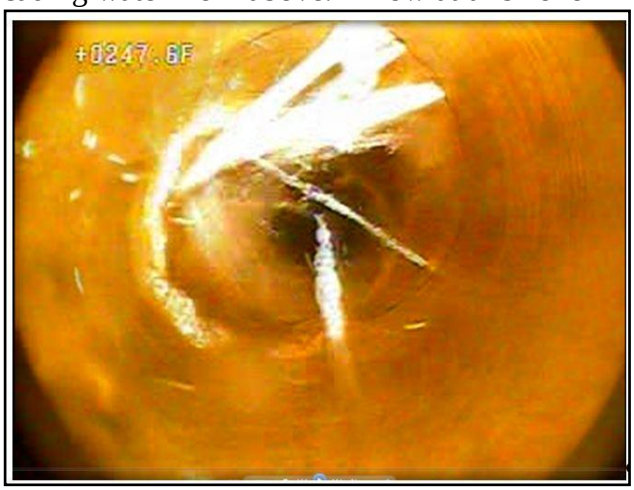

Figure 13. Video still image from July 17, 2012 showing cascading water and inflow jetting in from a subhorizontal fracture at 249 feet below land surface in the Gleason test hole, Bradford County, Pennsylvania (video presented in Appendix 4).

was evidenced by the movement of particles and filamentous bacteria on the video logs (Figure 14).

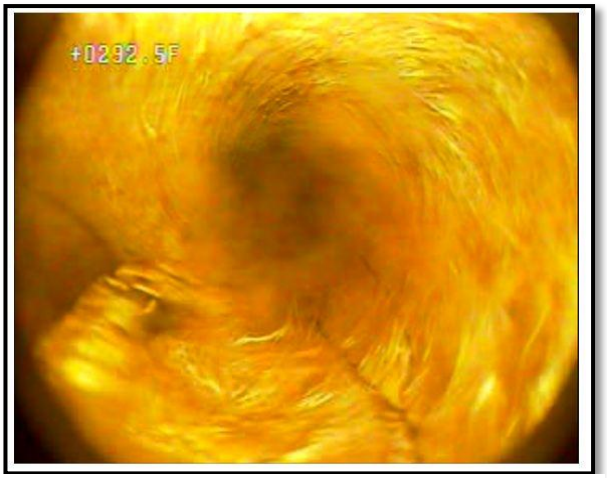

Figure 14. Video still images from October 2, 2012 showing filamentous bacteria growth near a high angle fracture at the water-bearing zone 294 feet below land surface in the Gleason test hole, Bradford County, Pennsylvania (videos presented in Appendix 4).

A water-bearing zone at 553 feet bls with a hydraulic head lower than the composite water level received about 1.2 gal/min of the downflow (Figure 11). The outflow zone at 553 feet bls was a subhorizontal fracture along a sandstone-claystone contact (Figure 15). Almost all of the remaining downflow (5.7 gal/min) was received by a highly transmissive zone with

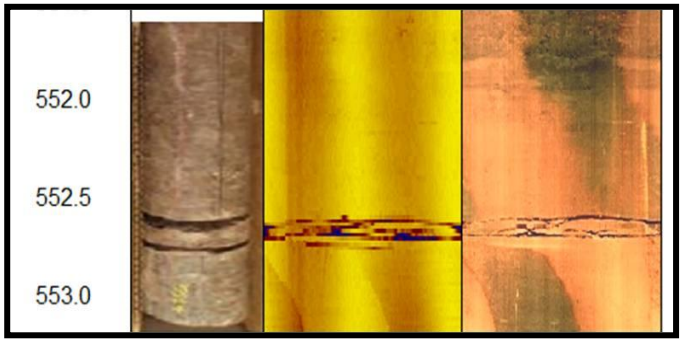

Figure 15. Core photograph and acoustic and optical televiewer images of subhorizontal fracture penetrated at 553 feet below land surface along a sandstone-claystone contact by the Gleason test hole, Bradford County, Pennsylvania.

a low hydraulic head at 661 feet. The 661-foot outflow zone was a subhorizontal fracture along bedding within an upward-fining sandstone unit (Figure 16). The temperature gradient measured in the test hole was isothermal between the composite water level and the 661-foot zone because of the large amount of downflow. Downward movement of bacterial particles and bacterial coating of the borehole wall in this interval and particle outflow into the 661-foot zone was observed on the video logs (Figure 17 and Appendix 4).

The small amount of remaining downflow (0.1 gal/min) was received at a water-bearing zone at 712 feet bls (Figure 18). The 712-foot outflow zone was a subhorizontal fractured zone at a contact between laminated siltstone above and sandstone with wavy bedding and a carbonaceous layer below. The temperature gradient sharply increased in the test-hole interval between the 661 and 712 feet bls zones reflecting the major loss of downflow at the 661 feet bls zone. Because the water-bearing zones at 553, 661, and 712 feet bls received outflow from the test hole under ambient conditions, the fluid resistivity and specific conductance logs were not useful in determining whether water from these zones might be fresh or saline. However, their high fracture transmissivity in contrast to the interval below, and their low hydraulic head relative to the water-bearing zones above and below, suggest that these zones are freshwater bearing.

Below the 712 feet bls zone to the bottom of the test hole, the waveform amplitudes on the sonic log increased and fracture density as identified on the image logs markedly decreased, no flow was detected by the flowmeters, and the temperature gradient approached the geothermal gradient, all of which indicated there was minimal fracture transmissivity in this interval (Figures 8 and 11). Seepage of saline water into the test hole was identified on the specific conductance logs

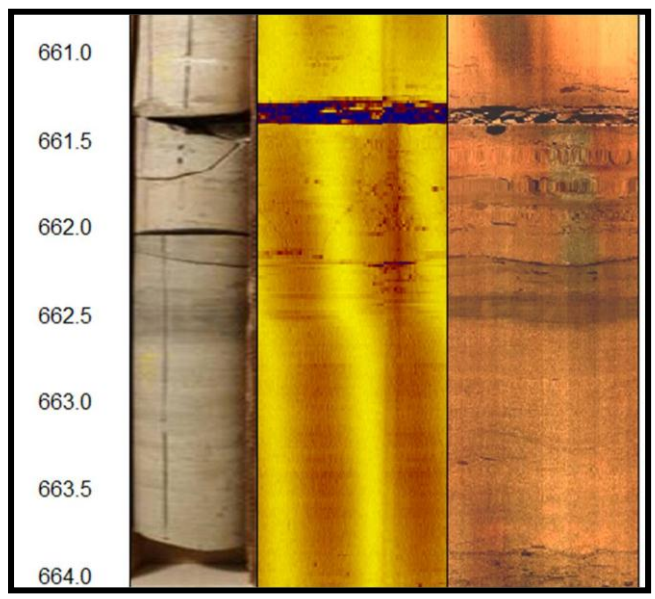

Figure 16. Core photograph and acoustic and optical televiewer images of a subhorizontal fracture penetrated at 661 feet below land surface by the Gleason test hole, Bradford County, Pennsylvania.

at 914 and 1,026 feet bls. The saline seepage zones were at subhorizontal fractures along bedding (Figure 19). As viewed on the video logs (Appendix 4), the saline inflow seeped

from distinct points along the fracture planes appearing as shimmering channels of downflow due to the density contrast with the test hole water (video still images, Figure 20). The hydraulic head in these very low transmissivity zones is uncertain, but the apparent slow upward movement of saline water in the test hole from the 914-foot zone to the 712-foot zone as documented by the time series of specific conductance logs collected between June 11 and October 2, 2012 (Figure 11) suggests an upward hydraulic gradient between these two zones.

Although not as well defined as the 914 and 1,026 foot zone seepage, a very small amount of saline seepage from the fracture at 1,311 feet bls might explain the elevated specific conductance of the test hole water in this interval of the hole. A small number of tiny particles appeared to be moving up the hole at this zone on the video log (Appendix 4).

Formation water resistivity was estimated for sandstone intervals with gamma values of less than 80 CPS (Figure 21) through application of Archie's Equation (Archie, 1942). Archie's Equation is an empirical relation that states:

$$R_w = R_t Ø^m$$

where

R_w is formation water resistivity (ohm-m),

R_t is true formation resistivity (ohm-m),

Ø is porosity (decimal), and

m is cementation factor (dimensionless).

Values of true formation resistivity were derived from the induction resistivity log. Values of porosity were derived from the neutron and density porosity logs. A cementation factor of 2.0, which is typical for consolidated sandstone, was assumed (Jorgensen and Petricola, 1994; Rider and Kennedy, 2011).

The application of Archie's Equation to estimate water quality is complicated by the variable clay content, presence of very fresh formation water in shallower intervals, low primary porosity, and discrete fractured nature of the bedrock. Due to the effects of surface conduction, Archie's Equation becomes invalid in a low-clay sandstone when fluid resistivity is greater than about 10 ohm-m (Hearst and Nelson, 1985). An increasing clay content increases surface conduction and lowers this threshold. The estimated formation water resistivities for the selected sandstone intervals were highly variable above 880 feet bls, ranging from less than 0.1 ohm-m to more than 10 ohm-m. However, below 880 feet bls, the estimated formation water resisitivities were all less than 1ohm-m. A formation water resistivity of less than 1 ohm-m at the ambient formation temperatures of 10°-15° Celsius, as indicated by the temperature logs, corresponds to a specific conductance of more than 12,200 to 13,300 μS/cm at 25° Celsius. The apparent transition from fresh to saline formation water at 880 feet bls that was estimated using this petrophysical approach is consistent with the fracture zone at 712 feet bls being freshwater bearing and the fracture zones at 914, 1,026 and 1,311 feet bls being saline-water bearing (Appendix 4).

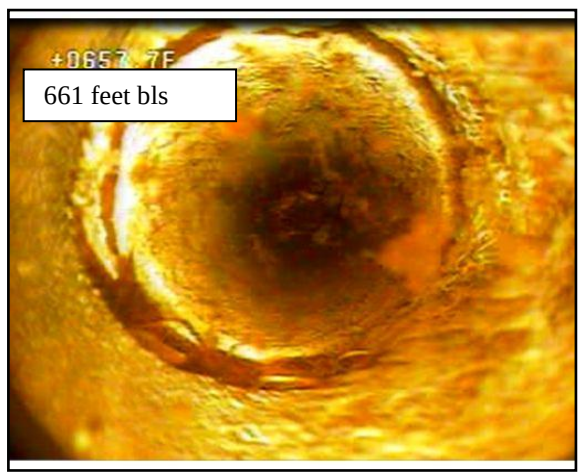

Figure 17. Video still image from October 2, 2012 showing freshwater outflow of rust-colored particles into a subhorizontal fracture penetrated at 661 feet below land surface by the Gleason test hole, Bradford County, Pennsylvania (videos presented in Appendix 4).

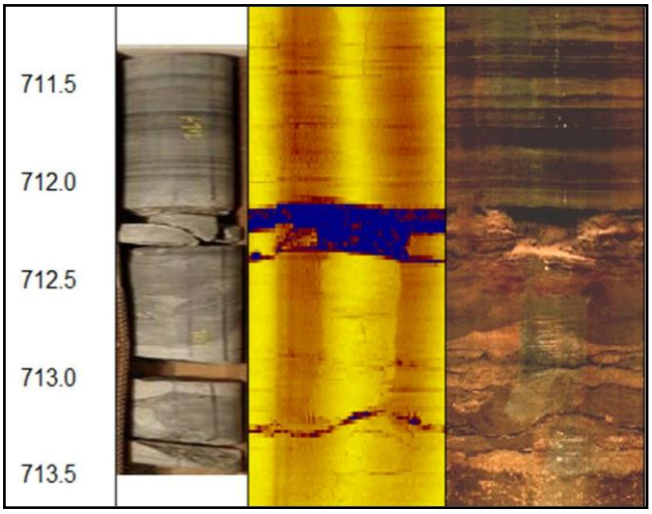

Figure 18. Core photograph, acoustic, and optical televiewer images of subhorizontal fracture penetrated at 712 feet below land surface by the Gleason test hole, Bradford County, Pennsylvania.

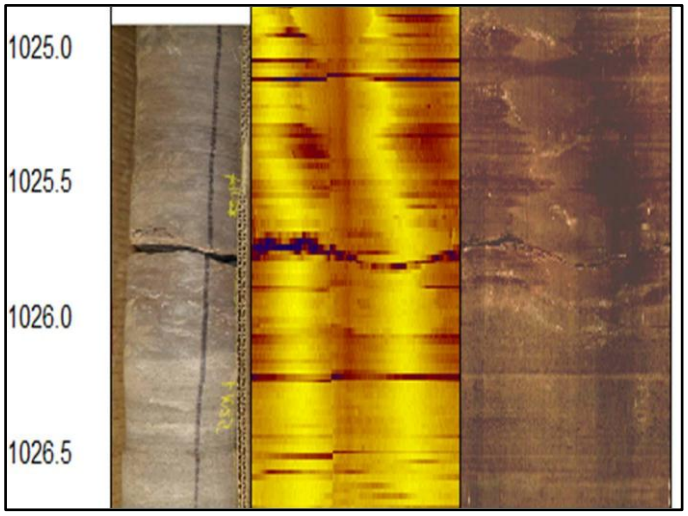

Figure 19. Core photograph and acoustic and optical televiewer images of subhorizontal fracture penetrated at about 1,026 feet below land surface by the Gleason test hole, Bradford County, Pennsylvania.

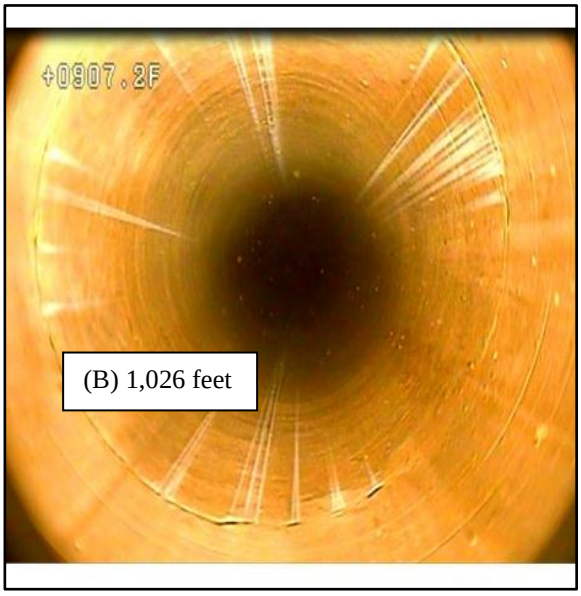

Figure 20. Video still images showing seepage of high-density saline water from subhorizontal fractures (A) at 914 below land surface on July 17, 2012 and (B) at 1,026 feet below land surface on October 2, 2012 in the Gleason test hole, Bradford County, Pennsylvania (videos presented in Appendix 4).

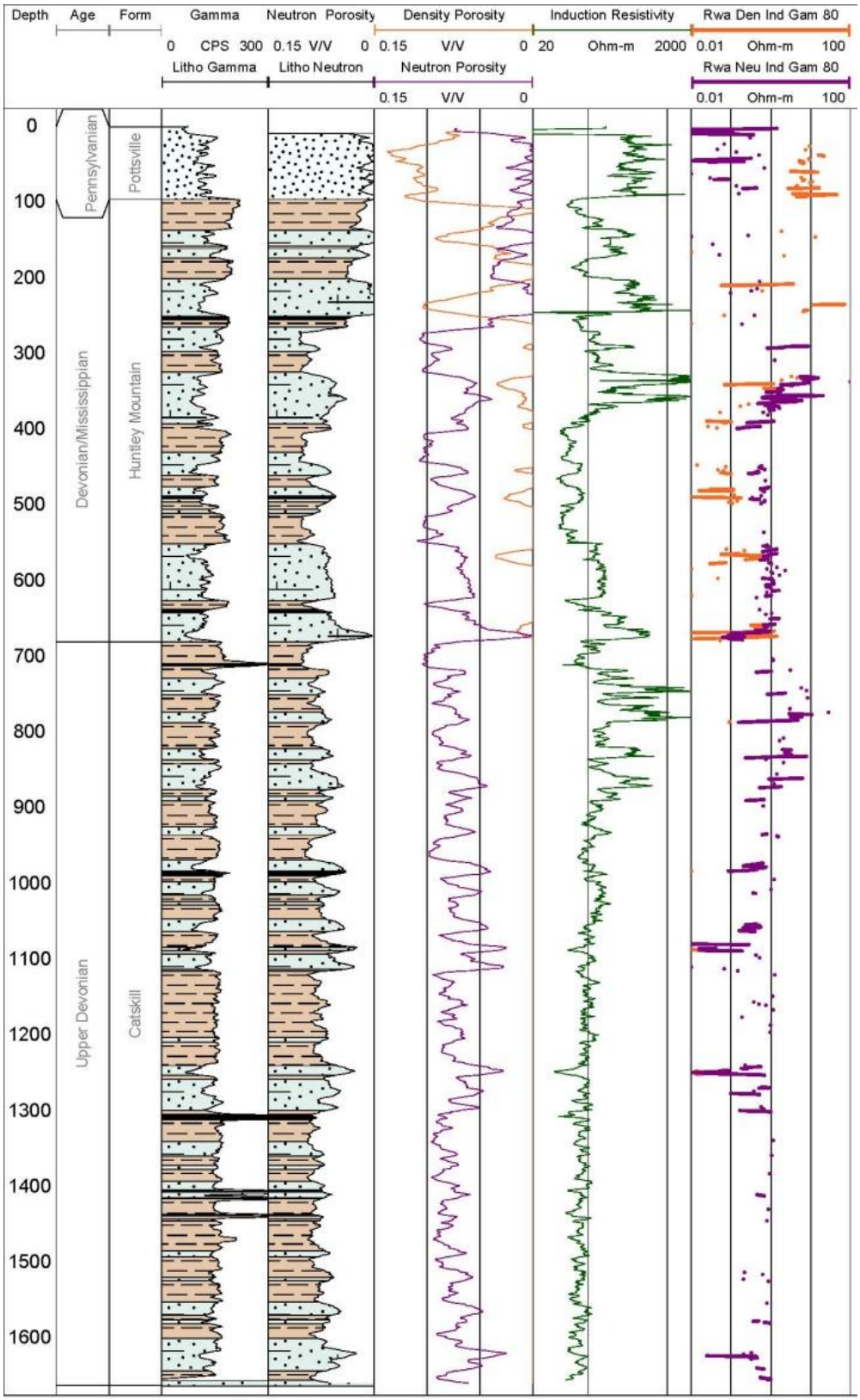

Figure 21. Logs of stratigraphy, lithology, gamma, neutron and density porosity, induction resistivity, and estimated formation water resisitivity for selected sandstone intervals penetrated by the Gleason test hole, Bradford County, Pennsylvania (explanation of log headings, units, and symbols are presented on p. 7).

WATER QUALITY

Quality of the water in the test hole was evaluated through analysis of the fluid logs, flowmeter logs, video, and five water-quality samples collected at specific depths. Differences in the chemistry of the water with depth in the test hole are the result of constituents in the water injected by the driller, water entering and exiting through fractures, chemical reactions between water and rock, and mixing of waters of differing chemical composition.

To characterize the water-quality differences related to hydrologic and geochemical processes, water samples were collected during June 19-20, 2012 from: (1) a depth of 550 feet bls to represent freshwater entering the hole between 52 and 294 feet bls and moving downward and exiting the test hole between 513 and 712 feet bls; (2) depths of 915 and 1,030 feet bls to represent small quantities of saline inflow from seeps identified at 914 and 1,026 ft bls; and (3) 1,500 feet bls to represent the relatively stagnant water below the saline seeps consisting largely of water injected into the hole after drilling.

During July 25-26, 2012, water moving up the test hole from the saline seep at 914 feet bls was resampled at a depth of 910 feet bls to characterize additional chemical constituents. The samples collected for selected analyses are summarized in Table 2 and results from the analyses of all the water samples and associated quality-assurance field blanks are listed in Appendix 2.

Water-bearing zones penetrated by the test hole at depths of 553, 661, and 712 feet bls were determined to be outflow zones, and because they were zones of outflow from the test hole under ambient conditions, the quality of water in those permeable zones could not be characterized by sampling with the point sampler technique used in this study.

During the 122 days that the test hole was open between June 4 and October 5, 2012, a filamentous bacterial biofilm grew in the hole. Videos of the test hole on July 17, 2012 showed a small growth at 294 ft bls, and on October 2, 2012 showed a dense growth between depths of about 290 to 712 ft bls (Figures 14 and 17). The inflow of water at and near 294 ft bls probably created conditions favorable for the establishment of bacteria and then the downward flow of water within the hole transported the bacteria to the major outflow zone at 661 ft bls where most of the bacteria exited the hole, with some continuing down to the deepest outflow zone at 712 ft bls. The bacteria were not sampled during the study, but based on their appearance in the video, are likely sulfur-metabolizing bacteria, whose growth is facilitated by the oxygenated water cascading from shallow zones above the water level in the test hole (Denise Akob, U.S. Geological Survey, oral commun., 2012).

Specific Conductance, Dissolved Solids, and Major Ions

Water moving down the test hole from the composite water level surface to the deepest outflow zone at 712 feet bls had a nearly constant specific conductance of 120 to 130 μS/cm at 25°C, as shown on all six traces of the specific-conductance log (Figure 11; Appendix 2, Table 1). A water sample collected at 550 feet bls indicates that the downward flow of water had a total dissolved-solids concentration of 87 mg/L, and can be categorized as “freshwater” (Figure 22). Below the outflow zone at 712 feet bls, the specific-conductance log showed inflows of water with high specific-conductance values at 914 and 1,026 feet bls. Water sampled from 915 and 1,030 feet bls during June 19-20, 2012 was moderately saline, with a total dissolved-solids concentration of about 5,000 mg/L; but 35 days later, total dissolved solids in a sample from 910 feet bls had increased to 12,700 mg/L, which is highly saline (Figure 22). The increase in dissolved-solids concentrations at about 910 feet bls likely

was caused by an inflow of water with dissolved solids in excess of 12,700 mg/L mixing with freshwater that initially was added by the driller to flush the test hole after drilling. Following completion of drilling, the test hole was flushed with fresh water from nearby Rundell Creek to remove any rock flour remaining in the hole. The injected water was not sent to the laboratory for chemical analysis, but the specific conductance of water taken from the creek was 28 µS/cm at 25°C. Thus, immediately after flushing, the test hole contained freshwater, some added by the driller and some from water-inflow zones between 50 and 294 feet bls, which was made more saline over time by the inflow from saline seeps at 914, 1,026, and possibly from one at 1,311 feet bls, as indicated by the water samples and specific-conductance logs collected from 7 to 120 days after drilling (Figure 11). From the time-series of fluid resistivity logs (Figure 11), it appeared unlikely that the test-hole water column had reached equilibrium with respect to total dissolved solids 120 days after drilling.

The major-ion composition of water samples from the test hole differed as illustrated on a trilinear diagram (Figure 23). The predominant ions in the sample collected at 550 feet bls were calcium and bicarbonate, which is typical of fresh groundwater from bedrock of Late Devonian to Pennsylvanian age in the Upper Susquehanna River Basin in Pennsylvania (Taylor, 1984, table 9). The composition of saline-water samples collected from 910, 915, and 1,030 feet bls is so similar that their symbols plot on top of each other in the trilinear diagram (Figure 23). The predominant ions in the saline-water samples are sodium, chloride, and calcium, similar to the composition of oil and gas well brines in western Pennsylvania reported by Dresel and Rose (2010). The predominant ions in the water sampled at 1,500 feet bls are calcium, sodium, chloride, and bicarbonate. The major-ion composition is intermediate between the saline water samples and the fresh-water sample (Figure 23). The chemical composition is consistent with the hypothesis that the water sampled at 1,500 feet bls is a mixture of freshwater used to flush the test hole and saline

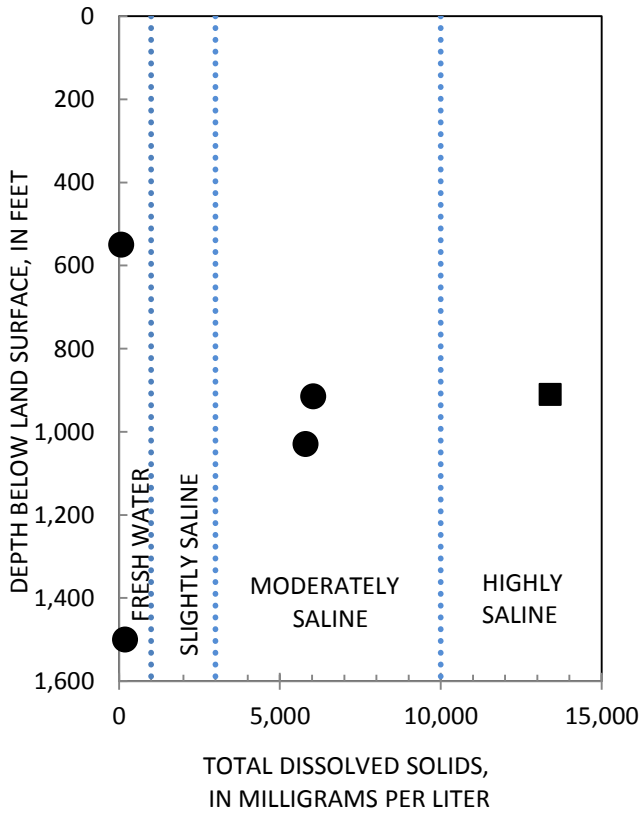

Figure 22. Total dissolved-solids concentration and designation of salinity of the water for point samples collected at selected depths in the Gleason test hole, Bradford County, Pennsylvania. Circles represent the June 19-20, 2012 samples and the square represents the July 25, 2012 sample. Definitions of fresh and saline water are from U.S.Geological Survey (2012).

water from seeps at 914, 1,026, and possibly 1,311 feet bls. Very low sulfate concentrations in all samples (less than 9 mg/L) allow barium, which would precipitate as barite in the presence of sulfate, to reach high levels (see section on trace constituents).

Quality-assurance samples showed that calcium was the only major ion detected in field blanks (Appendix 2, table 8). It was detected at the reporting level of 0.022 mg/L, much below concentrations found in the environmental samples.

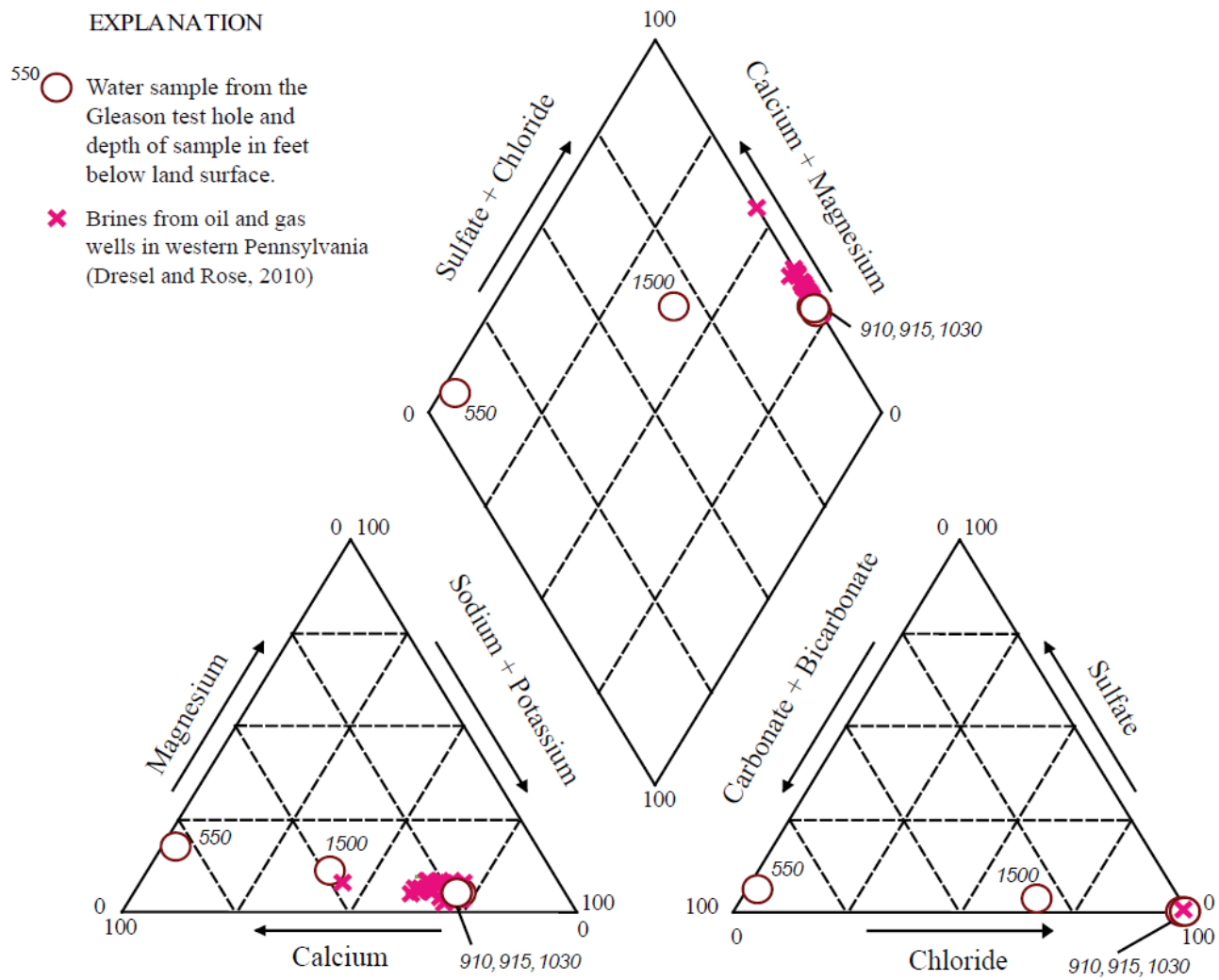

Figure 23. Trilinear diagram depicting the major-ion composition of five depth-dependent water samples collected from the Gleason test hole, Bradford County, Pennsylvania.

Trace Constituents and Radiochemicals

Concentrations of 23 trace constituents, gross alpha radioactivity, and gross beta radioactivity analyzed in filtered water samples from the Gleason test hole are listed in Appendix 2, Table 2. Metals and other trace constituents sampled from the five depths are plotted in Figure 24. The trace metals are arranged on the x-axis of the graph in order of largest to smallest concentrations that were present in the saline-water sample from 1,030 feet bls. Concentrations of trace metals reported as "less-than" values in Appendix 2, Table 2 were plotted at concentrations equal to one half of their reporting limit. Less-than values were greater than reported concentrations in a few samples for some metals (aluminum, copper, antimony, and lead). On this graph, parallel lines indicate waters of similar trace-metal composition, as shown by the lines representing saline waters sampled at 910, 915, and 1,030 feet bls.

In all samples, strontium, bromide, barium, lithium, iron, manganese, zinc, and fluoride were predominant trace constituents. The saline water samples from 910, 915, and 1,030 feet bls had higher concentrations of trace constituents than the freshwater samples, except for aluminum, uranium, chromium, copper, lead, and beryllium. Some concentrations were substantially elevated in the saline water samples relative to the freshwater at 550 feet bls, including many of the trace constituents

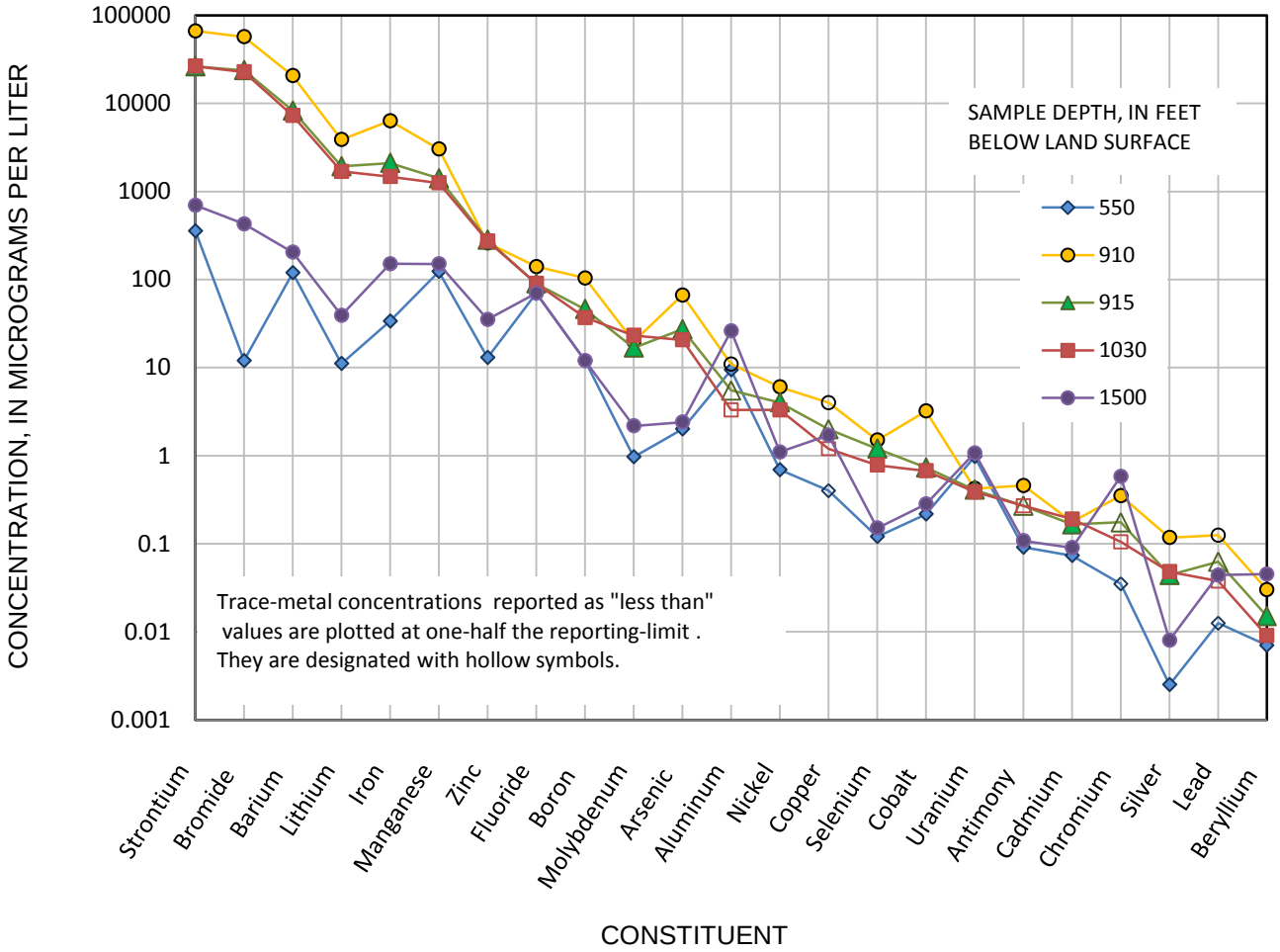

Figure 24. Concentrations of metals and other trace constituents in water sampled from specific depths in the Gleason test hole, Bradford County, Pennsylvania (non-detects for a few constituents are shown as half the detection level).

that have been shown to be elevated in the brines produced from oil and gas wells in western Pennsylvania (Dresel and Rose, 2010), and in Marcellus flowback and produced waters (Hayes, 2009; Haluszczak and others, 2013; Chapman and others 2012). Constituents that were present at concentrations at least 10-times greater in the saline water samples than in the freshwater at 550 feet bls were strontium, bromide, barium, lithium, iron, manganese, zinc, molybdenum, and arsenic. Figure 24 shows that the smallest concentrations of most trace metals were present in the fresh-water sample from 550 feet bls. Concentrations in the sample from 1,500 feet bls were greater than in the sample from 550 feet bls, but generally less than those in the saline-water samples from 910 to 1,030 feet bls, indicating that the chemistry of the water at 1,500 feet bls is consistent with a mixture of saline water with the freshwater initially added by the driller.

Quality-assurance samples showed that ten trace metals were detected in at least one of the two field blanks (Appendix 2, Table 8). Contamination was considered small (less than one third the concentration reported for environmental samples) for antimony, barium, manganese, and molybdenum; reported values of these constituents in environmental samples are probably minimally impacted from contamination. However, the concentrations of beryllium, cadmium, chromium, cobalt, iron, and nickel reported in Appendix 2, Table 2 (mostly for samples at 550 and 1,500 feet bls) could have been affected by contamination. The source of contamination was unknown, but was likely from the stainless-steel point sampler.

Bromide and chloride tend to be conservative constituents in groundwater that, once dissolved, are not easily lost from solution by precipitation, ion exchange, or other reactions (Davis and others, 1998). Thus, they are commonly used as tracers and indicators of dilution or mixing of waters, provided that the concentrations in the end-member waters differ. Mixing of waters causes a change in concentration of bromide or chloride in direct proportion to the mass loading from each end member. In the Gleason test hole, concentrations of bromide and chloride from samples at different depths illustrate the mixing of waters as shown by points that fall along the straight line in Figure 25. The bromide and chloride concentrations in the sample from 1,500 feet bls can be explained by a mixing within the test hole of about 99.25 percent freshwater of composition similar to that sampled at 550 feet bls and only 0.75 percent saline water similar to that sampled from 910 feet bls.

Also shown on Figure 25 is the median concentration of bromide and chloride from 40 brines analyzed from oil and gas fields in western Pennsylvania (Dresel and Rose, 2010) and from 7 samples of flowback water from Marcellus Shale gas wells samples by Hayes (2009) and reported by Haluszczak and others (2013, table 1). Extrapolating the mixing line on Figure 24 through these points indicates that the concentrations of bromide and chloride in the saline samples from depths of 910, 915, and 1,030 would be difficult to distinguish from theoretical mixtures of freshwater similar to that sampled at 550 ft bls with brines from the oil and gas fields or flowback-type waters.

Radiochemical analyses indicated that the saline water samples were elevated in both gross alpha particle and gross beta particle activity relative to the freshwater samples (Appendix 2, Table 2). Gross alpha and beta particle activities are measures of the radioactivity in a water sample attributable to the decay of alpha- or beta-emitting elements, respectively. Gross alpha was as high as 80 pCi/L in the saline water sample from 1,030 feet bls, exceeding the drinking water MCL of 15 pCi/L (U.S. Environmental Protection Agency, 2009). It is likely that the high gross alpha-particle activity indicates that radium-226 is elevated in the sample. Radium-226 is known to be elevated in brines (Haluszczak and others, 2013; Rowan and others, 2011), and gross alpha

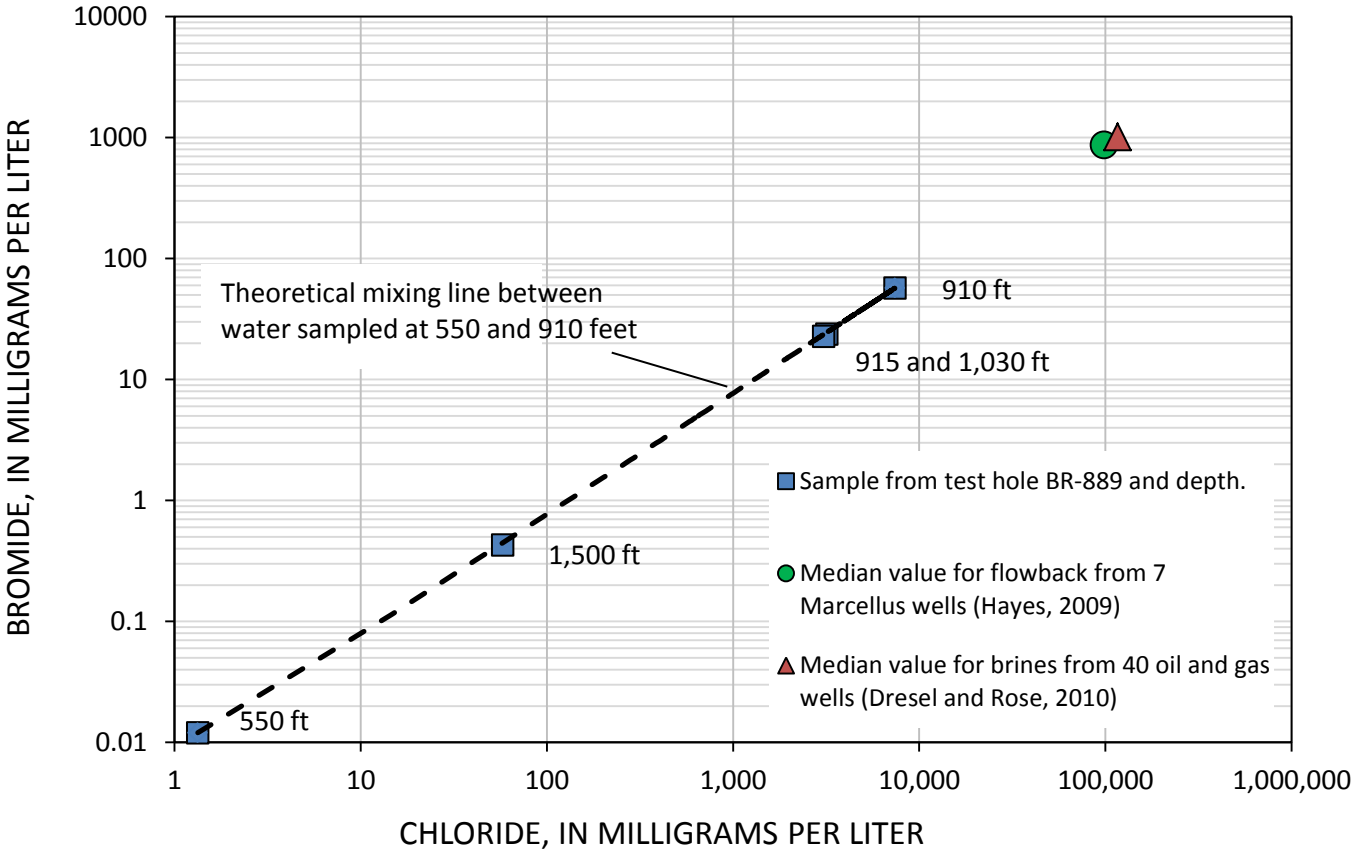

Figure 25. Relation between bromide and chloride concentrations in depth-dependent samples from the Gleason test hole, Bradford County, Pennsylvania.

particle activity has been shown to be directly related to radium-226 activity in southeastern Pennsylvania (Sloto, 2000). Quality-assurance samples showed that neither gross alpha nor beta activity was detected in field blanks (Appendix 2, Table 8).

Organic Constituents and Nutrients

Because the video log of the test hole showed a dense, milky-looking dense substance flowing into the well at 914 feet bls, a sample was collected at that depth and analyzed for additional constituents -- volatile organic compounds (VOCs) and semivolatile organic compounds (SVOCs), other organic constituents, nutrients, and strontium isotopes (discussed in later section). Results of those analyses are listed in Appendix 2, Tables 4-7. The only VOCs or SVOCs that were quantified without qualification were Bis(2-ethylhexyl) phthalate at 14 µg/L and Di-n-butyl phthalate at 8.3 µg/L. They were not detected in field or laboratory blanks, but are common laboratory contaminants that should be interpreted with caution (Environmental Protection Agency, 1992, p. 249-252). Surfactants (methylene blue active substances) were also detected at a concentration of 0.24 mg/L and all the nitrogen (1.55 mg/L as N) was in the form of ammonia. Toluene concentration was reported as an estimated value of 0.62 µg/L and diethyl phthalate was detected, but at a concentration too small to accurately report. Acetone, benzyl alcohol, and diesel range organics (C10-C36) were detected; however they were also detected in the field or laboratory blank, indicating the likelihood of contamination. The origin of these trace concentrations of organic substances and surfactants in the sample is not known, but the analyses indicate that the milky-looking inflow to the test hole likely is predominantly a dense, saline-water seep of apparent natural origin.

GASES AND STABLE ISOTOPES

The composition of gas was analyzed from samples of the rock core and groundwater. Stable isotopes were also analyzed to evaluate the isotopic signatures of hydrocarbon gases, water, and some dissolved solutes. The laboratory report for the analysis of gas composition and stable isotopes contains the following information: 1) molecular gas composition, which shows relative concentrations of selected saturated hydrocarbons (alkanes or paraffins) and associated structural isomers including methane (C_1), ethane (C_2), propane (C_3), *n*-butane and isobutane (C_4), pentane, isopentane, and neopentane (C_5), and hexane with traces of four other isomers (C_6); 2) nonhydrocarbon gases including helium, hydrogen, carbon dioxide, and nitrogen; and 3) stable carbon and hydrogen isotopes of methane, known as delta carbon-13 or $\delta^{13}C_{CH4}$ and delta deuterium or δD_{CH4}. For additional explanation of nomenclature, see Terms at the end of this report.

Composition of Gas Extracted from Core

Samples of carbonaceous bedrock were taken from the core at depths of 255.0, 641.6, 713.1, and 1,309.8 feet bls for analysis of gas composition and stable isotopes of carbon and hydrogen (Table 3).

Methane, ethane, and propane were the predominant hydrocarbons extracted from the four core samples. The ratio of methane to the higher chain hydrocarbons (C_1/C_2+) ranged from 0.25 to 7.6, which is indicative of thermogenic gases and is much smaller than the C_1/C_2+ ratio for gases in any of the water samples from the test hole (Figure 26).

The shallowest three core samples had insufficient gas to determine methane isotopes. The sample at 1,309.8 feet bls yielded -34.36 parts per thousand (per mil, ‰) $\delta^{13}C_{CH4}$ and -195.9 per mil δD_{CH4} (Appendix 2, Table 9), placing the gas in the range of thermogenic methane (Figure 27).

Table 3. Depths and description of samples taken from core of the Gleason test hole, Bradford County, Pennsylvania. [Abbreviations are explained in Appendix 1]

Sample No.	Depth (feet)	Formation	Lithology
57855-1-1	255.0	Huntley Mountain	254.9-256.2 feet: INTERLAMINATED SAND AND SILT: Sandstone, medium dark grey N4 with organics, coaly zone (sampled for isotope analysis) up to 0.25 in. thick with pyrite nodules up to an inch thick, interlayered with claystone, silt and vfL sands, visible pyrite crystals.
57855-1-2	641.6	Huntley Mountain	638.6 to 643.6 feet: SANDSTONE: Sandstone, fU, N4/N5, non-calcareous, some crossbeds, darker downward, 641.5-643.6 feet common organics, pyrite. Coaly organics at 641.6 feet (sampled for isotope analysis). Abundant organics in lower two feet; 643-651 ft unbroken.
57855-1-3	713.1	Catskill	709.0 to 714.7 feet: SILTSTONE: Siltstone, N3, fL-fU, with minor sand zones, sands at 708.7, 709.1, 709.4, 713-713.4, 713.5-713.7 feet with wavy contact and sand diapir. Calcareous. Abundant coal at 713.1 feet (sampled for isotope analysis). Calcareous dots at 713.6-714.5 feet Clayey fracture at 714.5 feet, about 2 mm all chewed up!
57855-1-4	1,309.8	Catskill	1,309.2 to 1,310.3 feet: CLAYSTONE: Claystone with organics, flakey, sulfur smell. Coaly lens at 1,309.8 feet, (sampled for isotope analysis). Last 0.4 feet is calcareous nodules, grey with sand.

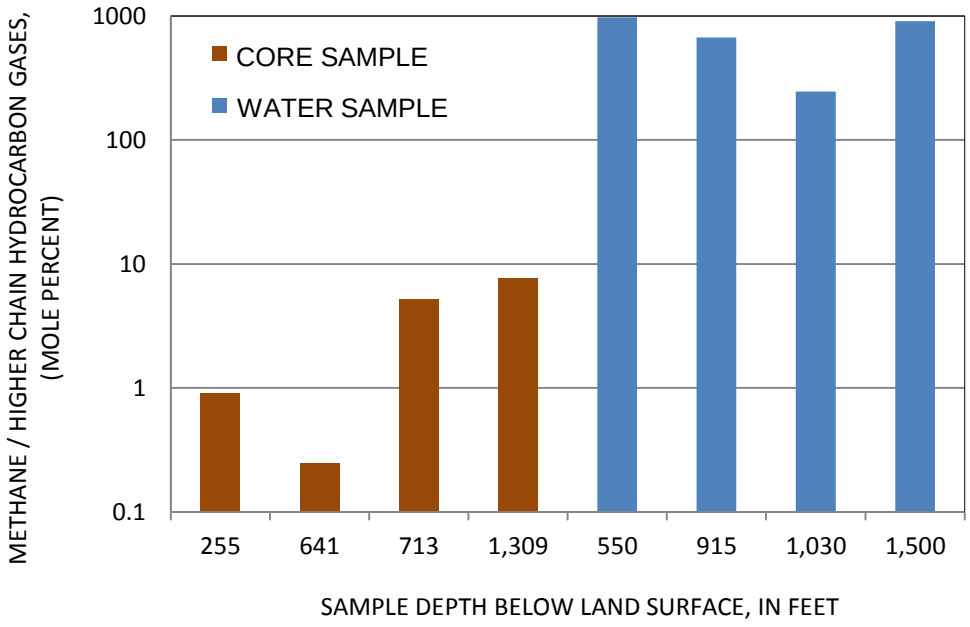

Figure 26. Ratios of methane to higher chain hydrocarbon gases from samples of rock core and water samples collected at various depths in the Gleason test hole, Bradford County, Pennsylvania.

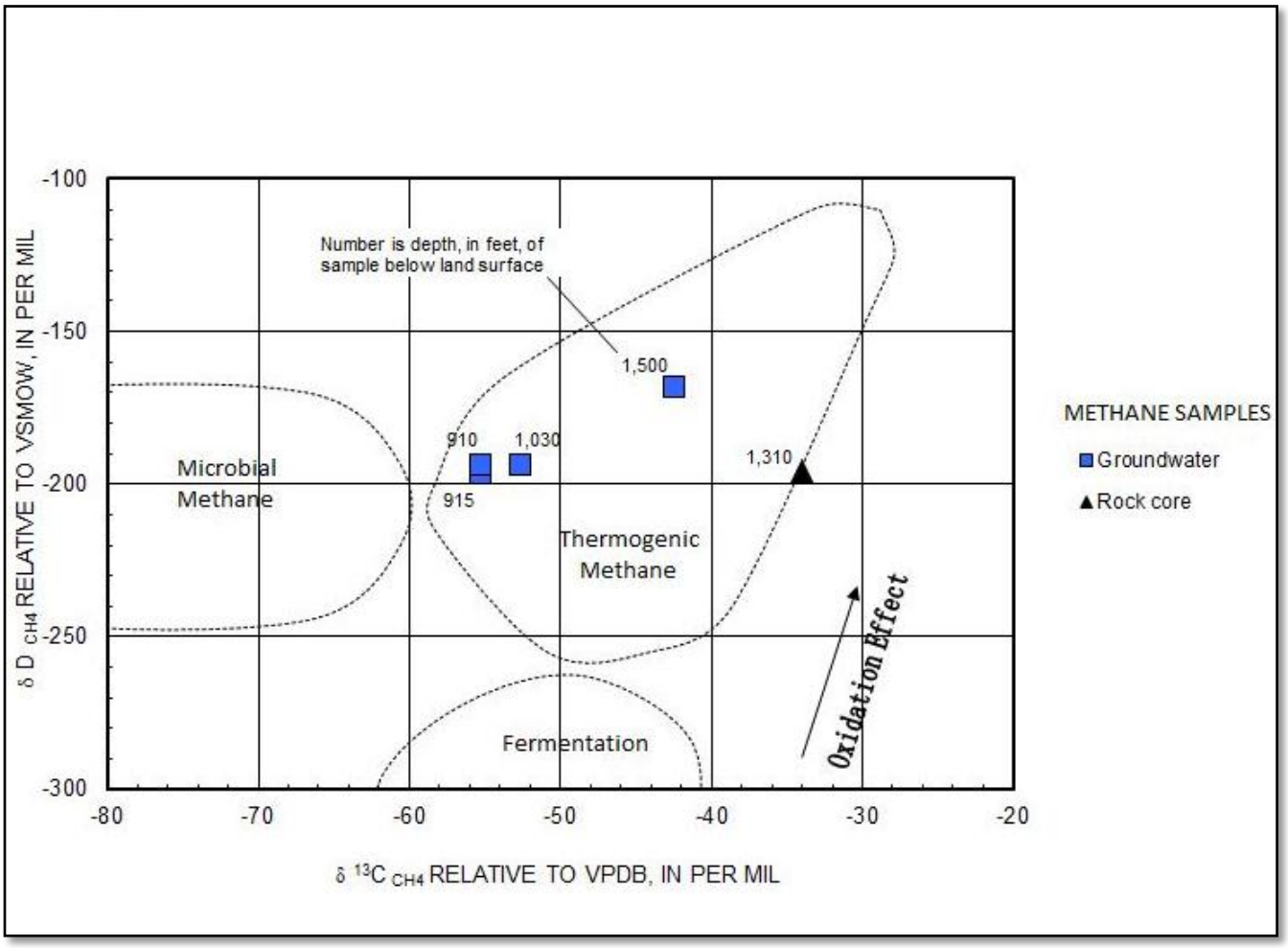

Figure 27. Stable carbon and hydrogen isotopic ratios for methane extracted from a carbonaceous zone in the rock core and from four specific-depth water samples in the Gleason test hole, Bradford County, Pennsylvania. Designated thermogenic, microbial, and fermentation origin fields from Breen and others (2007), modified from Coleman and others (1993).

Concentrations of Dissolved Gas and Stable Isotopes in Water

The concentrations of dissolved gases measured in five groundwater samples are given in Appendix 2, Table 3. Concentrations are reported as mole percent of gas in the headspace extracted from water, except for methane and ethane, which are also reported as mg/L of gas dissolved in water. Methane concentrations in groundwater were barely detectable (0.0003 mg/L) in the freshwater sample from 550 feet bls, and ranged from 7.8 to 37 mg/L in samples of saline water collected at 910, 915, and 1,030 feet bls. Concentrations of ethane and other hydrocarbon gases were much smaller than methane concentrations. Ratios of the concentration of methane to the sum of the higher-chain hydrocarbon gases C_1/C_2+ (in mole percent) ranged from 258 to 994 in groundwater samples, which is much greater than the range (.25 to 7.6) for gases extracted from the 4 samples of rock core (Figure 26). Ratios less than 100 (Osborn and others, 2011) or 1,000 (Révész and others, 2010) have been used to typify methane of thermogenic origin.

The isotopic analyses of four groundwater samples are listed in Appendix 2, Table 4. Stable isotope ratios were determined for $\delta^{13}C$ in methane and ethane, δD in methane and water, $\delta^{18}O$ in water, and $^{87}Sr/^{86}Sr$. For water

samples with sufficient methane for analysis, $\delta^{13}C_{CH4}$ ranged from -42.5 to -55.34 per mil and δD_{CH4} ranged from -168 to -196.6 per mil (figure 27). For water samples with sufficient ethane, $\delta^{13}C_{C2H6}$ ranged from -39.7 to -52.4 per mil. These analyses showed: (1) the values of both $\delta^{13}C_{CH4}$ and δD_{CH4} became greater (less negative) as the groundwater sample depth increased, and (2) the $\delta^{13}C$ values for methane were always less than for ethane. The relation between sample depth and $\delta^{13}C_{gas}$ values is shown in Figure 28 for methane and ethane in groundwater and for methane extracted from a carbonaceous section of core sample at 1,310 feet bls.

The isotopic values for methane ($\delta^{13}C_{CH4}$ and δD_{CH4}) from the four groundwater samples are characteristic of gases with a thermogenic origin (Figure 27) according to the classification of Coleman and others (1993). The isotopic analysis of $\delta^{13}C_{CH4}$ and δD_{CH4} for methane extracted from a core sample at 1,310 feet bls also indicates a thermogenic origin, with $\delta^{13}C_{CH4}$ values substantially less negative than any of the water samples (Figure 27).

Isotopic values for water (δD_{H2O} and $\delta^{18}O_{H2O}$) were analyzed for the groundwater sample of saline water collected at 910 feet bls for comparison to the local meteoric water line (Kendall and Coplen, 2001). The results of the analyses (δD_{H2O} = -60.9 per mil and $\delta^{18}O_{H2O}$ = -8.9 per mil) put the sample on the local meteoric water line, indicating that, although saline, the water recharged during post-glacial times and likely became saline by dissolving solutes from the rock or mixing with a small quantity of brine.

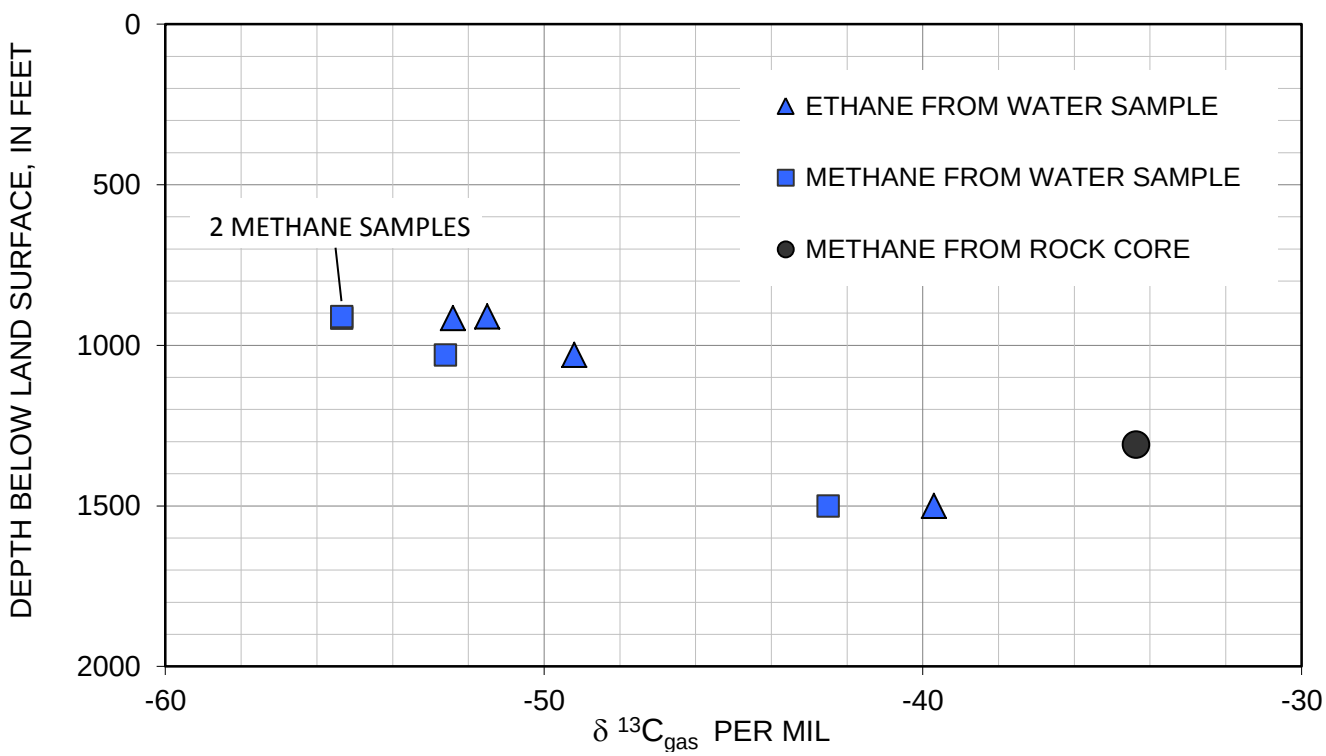

Figure 28. Relation between sample depth and δ13C values for methane and ethane in groundwater and from a carbonaceous zone in the rock core at 1,310 feet below land surface in the Gleason test hole, Bradford County, Pennsylvania

The isotopic ratio of strontium-87 to strontium-86 ($^{87}Sr/^{86}Sr$) was analyzed for the groundwater sample of water collected at 910 feet bls to provide basic data for this source of saline water from the Catskill Formation (Appendix 2, Table 4). Waters from differing sources may have distinct strontium isotopic ratios that can be used to identify those sources and evaluate mixing. The $^{87}Sr/^{86}Sr$ ratio for the sample was 0.71416, which is within the range of values of groundwater from the Catskill Formation in northeastern Pennsylvania reported by Vengosh and others (2011), and is substantially greater than values of produced waters from the Marcellus Formation reported by Chapman and others (2012).

INSIGHTS INTO ACTIVE AND RESTRICTED GROUNDWATER FLOW

The geohydrologic and water-quality characterization of the Gleason test hole provided insights into the conceptualization of the active and restricted groundwater-flow systems in the fractured bedrock of Mississippian and Late Devonian age in this area of intensive shale-gas development. Although the test hole was only one observation point, its depth of 1,664 feet bls provided new information on the distribution and character of freshwater in active-flow zones and saline water in restricted-flow zones.

The test hole was in an upland recharge setting in the headwaters of the Tioga River watershed on Armenia Mountain. The high topographic relief in this setting drives groundwater laterally and vertically downward along an interconnected fracture network in the sandstone-dominated bedrock to a depth of about 700 to 900 feet bls. This depth of active circulation was consistent with the deepest occurrence of freshwater at about 800 feet bls reported during gas-well drilling in bordering counties to the north in New York (Williams, 2010). Shallower depths of freshwater circulation, on the order of 200 feet or less below land surface, have been documented for valley settings in the region (Williams, 2010; Williams and others, 1998; Lohman, 1939, p.108).

The fractures at 661 and 712 feet bls likely are fresh-water bearing and appeared to serve as subsurface drains for the active groundwater flow system. Depths of these lower hydraulic-head zones straddle the depth of the gradational stratigraphic contact between the Huntley Mountain and Catskill Formations at 682 feet bls. Petrophysical-log analysis indicated that the formation water below 880 feet bls was saline. Saline-water inflows were verified by groundwater samples of seepage from zones at 914 and 1,026 feet bls. Those zones appeared to have higher hydraulic head than the drains of the active flow system (at 661 and 712 feet bls) as evidenced by upward movement of saline water shown by successive logs of fluid resistivity in the test hole.

The depth of active freshwater circulation corresponds to the depth of significant fracturing as documented with core and televiewer logs. Fractures are most common in the Pottsville and Huntley Mountain Formations to a depth of about 150 feet bls, and are present, but less common, throughout the Huntley Mountain Formation and uppermost part of the Catskill Formation. Few fractures were penetrated in the Catskill Formation below 800 feet bls.

The depth of freshwater circulation was below the altitude of the surface-water drains for the local groundwater system but above the altitude of the surface-water drains for the more regional groundwater system (Figures 1 and 29) The deepest freshwater-outflow zone penetrated by the test hole at 712 feet bls was about 400 feet below the altitude of Rathbone Creek to the north and Rundell Creek to the south, which are the nearest drains for the local groundwater system, and was also more than 150 feet below the altitude of the confluence of Rundell Creek

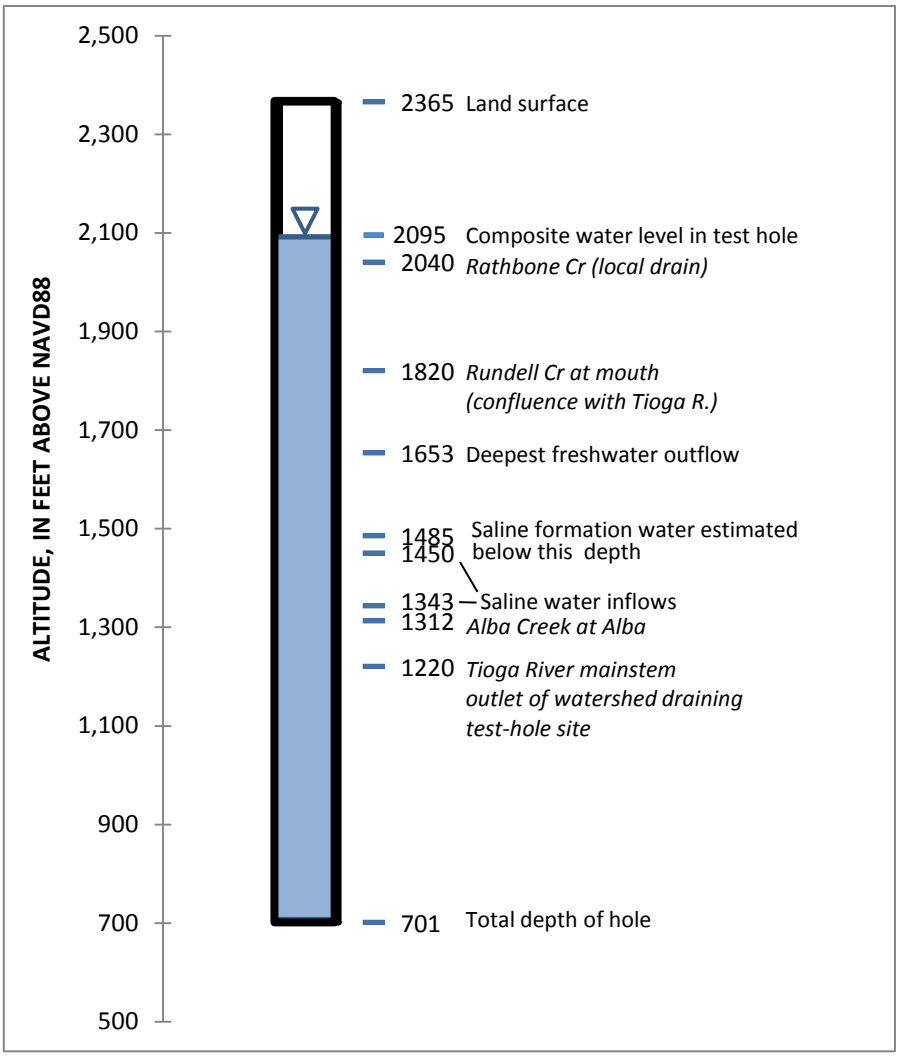

Figure 29. Schematic diagram showing altitudes of water-bearing zones and altitudes of stream drainage in the vicintiy of the Gleason test hole, Bradford County, Pennsylvania.

with the main stem of Tioga River. However, the freshwater-outflow zone was several hundred feet above the altitude of Tioga River at the outlet of the watershed to the west at which point it collects all surface runoff from its headwaters on Armenia Mountain. The freshwater-outflow zone also was several hundred feet above the altitude of Alba Creek at Alba near the base of the steep topographic slope to the east.

Saline water sampled from this upland test hole has similar characteristics to brine reported by Dresel and Rose (2010) that has been diluted by mixing with fresh water, and methane in saline-water samples had similar isotopic signatures to gases from Upper Devonian rocks reported by Osborn and others (2011) and Baldassare (2011). The presence of thermogenic methane gas with the saline water may be indicative of restricted flow zones that are not being continuously flushed by active circulation of fresh water or a mixture of small amounts of methane-containing brine with freshwater.

SUMMARY

An integrated analysis of core, geophysical logs, gas isotopes, and specific-depth water-quality samples from a 1,664 foot deep test hole was used to characterize the stratigraphy, water-bearing zones, and groundwater quality at a site in western Bradford County, Pennsylvania. The study was completed as a cooperative effort between the Pennsylvania Department of Natural Resources, Bureau of Topographic and Geologic Survey (BTGS) and the U.S. Geological Survey (USGS). The multi-disciplinary characterization of the test hole was done to provide information to aid the bedrock mapping of the Troy 7.5-minute quadrangle by BTGS, and to help quantify the depth and character of fresh and saline groundwater in an area of shale-gas exploration.

The Gleason test hole was drilled in 2012 by coring at an upland location in the headwaters of the Tioga River on Armenia Mountain. Core collected from the test hole is stored in the BTGS core library in Middletown, Pennsylvania, and is available for examination upon request. Evaluation of the core showed the drill penetrated 98 feet of the Pottsville Formation of Mississippian age, 584 feet of the Huntley Mountain Formation of Mississippian and Devonian age, and 982 feet of Catskill Formation of Late Devonian age. The Pottsville was identified by the predominance of sandstone, and the Catskill was distinguished from the Huntley Mountain Formation on the basis of more abundant and thicker packages of red and grayish-red interbedded sandstones, claystones, and siltstones. Bedding in the bedrock formations was planar with noticeable crossbedding. Bedding orientation as determined from analysis of the optical televiewer log, had a mean strike of 194 degrees with a mean dip of three degrees to the northwest, which was consistent with the test-hole location on the southern limb of the Blossburg Syncline.

The depth of fractures was determined through analysis of the core, caliper, sonic, and televiewer logs. The fractures were most commonly penetrated (about 32 fractures per 50 feet) in the Pottsville and Huntley Mountain Formations to a depth of about 150 feet, and were present, but much less frequent (about 6 fractures per 50 feet) throughout the Huntley Mountain Formation and uppermost part of the Catskill Formation. Few fractures were identified the Catskill Formation below 800 feet bls. Most of the fractures are bedding-parallel fractures and orientations of the less common steeply-dipping fractures are consistent with the regional primary and secondary joint set with a strike of 150 and 070 respectively (Behr and Hand, 2013). The orientation of breakouts discontinuously present in selected mudstone units between 785 to 1475 feet bls indicated that the direction of maximum horizontal stress is 070, which is consistent with regional estimates.

The test hole penetrated multiple water-bearing zones with differing hydraulic heads and transmissivity. Freshwater circulates downward along an interconnected fracture network in the bedrock to a depth of about 700 to 900 feet bls. The depths of water-bearing zones were identified by geophysical-log analysis and, for inflow zones, verified by groundwater sampling at specific depths. The composite water level in the test hole was about 270 bls in summer 2012. During the period of investigation from June to October 2012, fresh groundwater cascaded into the hole from water-bearing zones at 50 to 52, 96 to 106, 148 to 154, 192, 225, and 249 feet bls. More freshwater entered at 294 feet bls, contributing to a cumulative downward flow from these zones of about 7 gal/min. The water moved downward and exited the hole through fractures at 553, 661, and 712 feet bls. A groundwater sample collected at 550 feet bls showed that the downward flow was freshwater, having a

dissolved-solids concentration of 87 mg/L. The quality of water in the fracture zones at 553, 661, and 712 feet bls could not be sampled with the wireline point sampler used in the study because these zones were receiving outflow rather than producing water during the period the test hole was open. However, their relatively substantial fracture transmissivity and low hydraulic head in contrast to the interval below suggested that these zones are freshwater bearing.

The transition of fresh to saline formation water below 880 feet bls as determined using a petrophysical-log approach was consistent with the distribution of freshwater and saline-water bearing fractures as determined by the integrated analysis of the geophysical logs and specific-depth water samples. A depth of active freshwater circulation of more than 800 feet in this high-relief upland setting in fractured sandstone-dominated clastic bedrock was also consistent with reported deepest fresh water penetrated during gas-well drilling in bordering counties to the north in New York. The depth of active freshwater circulation was at an altitude below local streams near the Gleason test hole, but above the altitude of the main stem of Tioga River, which drains Armenia Mountain to the west, and the altitude of Alba Creek at Alba near the base of the steep topographic slope to the east.

Groundwater samples of saline-water inflows at 914 and 1,026 feet bls verified the presence of highly saline water with a minimum total dissolved solids concentration of 12,700 mg/L in the restricted flow system. As viewed on the video logs, the saline inflow from the two seeps appeared as shimmering, milky channels of downflow probably because of the density contrast with the water in the test hole. The hydraulic head in these very low transmissivity zones is uncertain but the apparent slow upward movement of saline water in the test hole from the 914-feet bls zone to the 712-feet bls zone, as documented by the time series of specific conductance logs, indicates an upward hydraulic gradient between these two zones.

Saline water sampled from this upland test hole has similar characteristics to brines reported by Dresel and Rose (2010) diluted by mixing with fresh water. The predominant ions in saline-water seeps were sodium, chloride, and calcium; the predominant ions in the freshwater samples were calcium and bicarbonate. The saline water samples had elevated concentrations of the trace constituents strontium, bromide, barium, lithium, iron, manganese, zinc, molybdenum, and arsenic and also gross alpha and gross beta radioactivity that were at least 10-times greater than in the freshwater sample from 550 feet bls. Gross alpha particle activity was as high as 80 pCi/L in the saline water.

Because the video log of the test hole showed a dense, milky looking substance flowing into the well at a saline inflow at 914 feet bls, an additional sample was collected and analyzed for organic constituents and nutrients. The analyses established that the milky looking inflow to the well likely is a dense saline-water seep of apparent natural origin that has relatively elevated ammonia concentrations and may contain low concentrations of surfactants. The only organics that were quantified without qualification were Bis(2-ethylhexyl) phthalate at14 μg/L and Di-n-butyl phthalate at 8.3 μg/L. Surfactants (methylene blue active substances) were detected at a concentration of 0.24 mg/L, and all the nitrogen (1.55 mg/L) was in the form of ammonia.

The gas analysis conducted on water and core samples contained information including: (1) composition of saturated hydrocarbons (alkanes or paraffins) and associated structural isomers: methane, ethane, propane-butane and isobutene, pentane, isopentane, neopentane, and hexane; (2) composition of nonhydrocarbon gases including helium, hydrogen, carbon dioxide, and nitrogen; and (3) ratios of stable carbon and hydrogen isotopes of methane. Methane concentrations were low (0.0003

mg/L) in the freshwater sample at 550 feet bls but higher (7.8 to 37 mg/L) in the saline groundwater samples from 910, 915, and 1,030 feet bls. Water sampled from 1,500 ft bls had 0.87 mg/L of methane. In four core samples, the ratio of methane to the higher chain hydrocarbons ranged from 0.25 to 7.6 indicating a thermogenic origin of the methane. In four water samples, the ratio of methane to the higher chain hydrocarbons ranged from 258 to 994, which is not definitive of either a thermogenic or biogenic (microbial) origin. Analyses of $\delta^{13}C_{CH4}$ and δD_{CH4} from the core sample at 1,309.8 feet bls, and water samples from 910, 915, and 1,030, and 1,500 ft bls indicate a thermogenic origin of methane.

ACKNOWLEDGMENTS

The authors gratefully acknowledge the following individuals for their expertise, insight, and significant contributions to the research on this project. The core samples chosen for gas isotope geochemistry were based on characteristics of similar lithologies in outcrops as seen in the field with and courtesy of Brent Wilson, Geoscience Coordinator, Chesapeake Energy Corporation–Oklahoma City, Oklahoma. Alton Anderson, Randall Conger, and Philip Bird of USGS collected the geophysical logs and borehole videos and assisted with groundwater sampling. USGS colleague reviews of the report were provided by Dennis Low and Roger Morin.

TERMS

Alkane: Chemical compounds that consist of only hydrogen and carbon atoms bonded exclusively by single linear bonds without any cycles or loops; also known as paraffins or saturated hydrocarbons.

British thermal unit (Btu): Traditional unit of energy equal to 1055 joules. Quantity of heat, about 252 calories, required to raise the temperature of one pound of water one degree Fahrenheit at a constant pressure of one atmosphere.

Carbon isotope of methane ($\delta^{13}C_{CH4}$): Stable carbon isotope $^{13}C/^{12}C$ composition ratio of methane, known as delta carbon-13, based on the international standard Vienna Pee Dee Belemnite (VPDB). Delta ^{13}C varies in time as a function of productivity, organic carbon burial, and vegetation type. Natural abundances of carbon-12 and carbon-13 are respectively 98.892 percent and 1.108 percent.

Hydrogen isotope of methane (δD_{CH4}): Stable hydrogen isotope $^{2}H/^{1}H$ composition ratio of methane, known as delta hydrogen-2 or deuterium, based on the international standard Vienna Standard Mean Ocean Water (VSMOW). Hydrogen-2 is ubiquitous in the terrestrial environment, has the largest mass difference between stable isotopes, is twice as heavy as hydrogen-1, and has the largest variation in stable isotope ratios in the environment.

Isomer: Compounds with the same molecular or chemical formula but different structural formulas (atomic arrangement and bonding). Structural isomerism (constitutional isomerism) forms when molecules with the same molecular formula bond together in different orders in alkanes with more than three carbon atoms. The simplest isomeric alkane contains carbon atoms that are arranged in a single chain with no branches (i.e. *n*-butane or "normal" butane). This chain of carbon atoms, however, may also be branched at one or more points.

Isotope: Atoms of the same element that have the same number of protons, but different numbers of neutrons and different masses.

Mole percent (mol. %): Mole fraction or molar percent of a substance is the ratio of the moles of a substance in a mixture to the total number of moles in the mixture. A mole is a unit of measurement used to express amounts of a chemical substance that contains as many elementary entities as there are atoms in 12 grams of pure carbon-12. In chemistry and physics, the Avogadro constant (Avogadro's number) = 6.02×10^{23} mol^{-1} and is the number of atoms in a gram atom, or the number of molecules in a gram molecule, or the number of atoms or molecules in one mole of a given substance. It is one of the base units in the International System of Units.

Paraffin: The technical name for an alkane (saturated hydrocarbon), specifically referring to a linear, or normal alkane. These hydrocarbons have the general formula C_nH_{2n+2}. The simplest paraffin molecule is methane, CH_4.

Pounds per square inch absolute (psia): The amount of pressure exerted on a fluid/gas measured in force per unit area of one square inch.

Saturated hydrocarbon: The simplest of the hydrocarbon species (alkanes) that are composed of single bonds and carry the full complement of hydrogen atoms. The general formula is C_nH_{2n+2} assuming non-cyclic structures.

Stable isotope: A form of an element that does not undergo radioactive decay at a measurable rate.

REFERENCES CITED

Archie, G. E., 1942, The electrical resistivity log as an aid in determining some reservoir characteristics: Transactions, American Institute of Mining, Metallurgical and Petroleum Engineers, v. 146, p. 54–62.

Baldassare, F. J., 2011, The origin of some natural gases in Permian through Devonian age systems in the Appalachian Basin & the relationship to incidents of stray gas migration, p. 64-68, *in* Proceedings of the technical workshops for the hydraulic fracturing study: chemical and analytical methods: U.S. Environmental Protection Agency, EPA 600/R-11/066, May 2011, 115 p.

Behr, Rose-Anna, and Hand, K. L., 2013, Bedrock geologic map of the Troy quadrangle, Bradford County, Pennsylvania: Pennsylvania Geological Survey, 4th ser., Open-File Report OFBM 13-01.0, 12 p. Portable Document Format (PDF)

Breen, K. J., Révész, Kinga, Baldassare, F. J., and McAuley, S. D., 2007, Natural gases in ground water near Tioga Junction, Tioga County, North-Central Pennsylvania – Occurrence and use of isotopes to determine origins, 2005: U.S. Geological Survey Scientific Investigations Report 2007-5085, 65 p. Portable Document Format (PDF). [http://pubs.usgs.gov/sir/2007/5085/pdf/sir2007-5085.pdf accessed March, 2013].

Brown, E.T., Green, S.J., and Sinha, K.P., 1981, The influence of rock anisotropy on hole deviation in rotary drilling—A review: International Journal of Rock Mechanics and Mining Sciences, v. 18, no. 5, p. 387-401.

Chapman, E. C., Capo, R. C., Stewart, B. W., Kirby, C. S., Hammack, R. W., Schroeder, K. T., and Edenborn, H. M., 2012, Geochemical and strontium isotope characterization of produced waters from Marcellus shale natural gas extraction: Environmental Science and Technology, v. 46, p. 3545-3553.

Coleman, D. D., Liu, C. L., Hackley, K. C., and Benson, L. J., 1993, Identification of landfill methane using carbon and hydrogen isotope analysis, *in* Proceedings, Sixteenth International Madison Waste Conference: Municipal & Industrial Waste, September 22-23, 1993: Department of Engineering Professional Development, University of Wisconsin-Madison, p. 303–314.

Davis, S. N., Whittemore, D. O., and Fabryka-Martin, J., 1998, Uses of chloride/bromide ratios in studies of potable water: Ground Water, v. 36, no 2, p. 338-350.

Dresel, P. E., and Rose, A. W., 2010, Chemistry and origin of oil and gas well brines in western Pennsylvania: Pennsylvania Geological Survey, 4th ser., Open-File Report OFOG 10–01.0, 48 p., Portable Document Format (PDF).

Environmental Protection Agency, 1992, Guidance for data useability in risk assessment (Part A), Office of Emergency and Remedial Response, Publication 9285.7-09A, PB92-963356, April 1992, 279 p., Portable Document Format (PDF). [*http://www.epa.gov/oswer/riskassessment/datause/parta.htm* accessed April, 2013].

Faill, R. T., compiler, 2011, Folds of Pennsylvania—GIS data and map: Pennsylvania Geological Survey, 4th ser., Open-File Report OFGG 11–01.0, scale 1:500,000.

Haluszczak, L. O., Rose, A. W., and Kump, L. R., 2013, Geochemical evaluation of flowback brine from Marcellus gas wells in Pennsylvania USA: Applied Geochemistry, v. 28, p 55-61

Hayes, T., 2009, Sampling and analysis of water streams associated with the development of Marcellus shale gas, *in* ALL Consulting, 2010, NY DEC SGEIS Information Requests and Industry Responses, Final Report for the Marcellus Shale Coalition: Gas Technology Institute, Des Plaines, IL, 356 p. Portable Document Format (PDF) [http://catskillcitizens.org/learnmore/20100916IOGAResponsetoDECChesapeake_IOGAResponsetoDEC.pdf accessed March 11, 2013]

Hearst, J.R. and Nelson, P.H., 1985, Well logging for physical properties, New York, McGraw-Hill, 571 p.

Hess, A. E., 1982, A heat-pulse flowmeter for measuring low velocities in boreholes: U.S. Geological Survey Open-File Report 82–699, 44 p. Portable Document Format (PDF) [*http://pubs.er.usgs.gov/usgspubs/ofr/ofr82699 accessed March, 2013].*

Johnson, C. D., 1996, Use of a borehole color video camera to identify lithologies, fractures, and borehole conditions in bedrock wells in the Mirror Lake Area, Grafton County, New Hampshire, *in* Morganwalp, D. W., and Aronson, D. A., eds., U.S. Geological Survey, Toxic Substance Hydrology Program Proceedings of the Technical Meeting, Colorado Springs, Colorado, September 20-24, 1993: U.S. Geological Survey Water-

Resources Investigations Report 94-4015, v. 1, p. 89-94. Portable Document Format (PDF). [*http://pubs.usgs.gov/wri/1994/4015/report.pdf*].

Jorgensen, D. G., and Petricola, M., 1994, Petrophysical analysis of geophysical logs of the National Drillng Company--U.S. Geological Survey ground-water research project for Abu Dhabi Emirate, United Arab Emirates: U.S. Geological Survey Water-Supply Paper 2417, 35 p.

Kelley, D. R., 1969, A summary of major geophysical logging methods: Pennsylvania Geological Survey, 4th ser., Mineral Resources Report 61, 82 p.

Kendall, C. and Coplen, T., 2001, Distribution of oxygen-18 and deuterium in river waters across the United States: Hydrologic Processes, v. 15, p. 1363–1393.

Keys, W. S., 1990, Borehole geophysics applied to ground-water investigations: U.S. Geological Survey Techniques of Water-Resources Investigations, book 2, chap. E2, p. 150.

Lohman, S. W., 1939, Ground Water in North-Central Pennsylvania: Pennsylvania Geological Survey, 4th Series, Bulletin W6, 219 p., 11 plates.

McLaurin, B. T., and Dodge, C. H., 2012, Bedrock geologic map of the Blossburg quadrangle, Tioga County, Pennsylvania: Pennsylvania Geological Survey, 4th ser., Open-File Report OFBM 12–01.0, 16 p. Portable Document Format (PDF).

Osborn, S. G., Vengosh, A., Warner, N. R., and Jackson, R. B., 2011, Methane contamination of drinking water accompanying gas-well drilling and hydraulic fracturing: Proc. Natl. Acad. Sci, USA 108: 8172–8176.

Pennsylvania Department of Environmental Protection, 2012, Gas well permit for horizontal gas well Fortuna Harris (01-004-02) M3H: Pennsylvania Department of Environmental Protection Northwest Regional Office, permit 015-20220, received December 12, 2008.

Révész, K. M., Breen, K. J., Baldassare, A. J., and Burruss, R. C., 2010, Carbon and hydrogen isotopic evidence for the origin of combustible gases in water-supply wells in north-central Pennsylvania: Applied Geochemistry, v. 27, pp. 361-375.

Rider, M., and Kennedy, M., 2011, The geological interpretation of well logs: Rider-French Consulting Limited, 3rd Edition, Bell and Bain, Glasgow, 432 p.

Rowan, E. L., Engle, M. A., Kirby, C. S., and Kraemer, T. F., 2011, Radium content of oil- and gas-field produced waters in the northern Appalachian Basin (USA)—Summary and discussion of data: U.S. Geological Survey Scientific Investigations Report 2011–5135, 31 p.

Sloto, R. A., 2000, Naturally occurring radionuclides in the ground water of southeastern Pennsylvania: U. S. Geological Survey Fact Sheet 012-00, 8 p.

Taylor, L. E., 1984, Groundwater resources of the Upper Susquehanna River basin, Pennsylvania: Pennsylvania Geological Survey, 4th ser., Water Resource Report 58, 136 p.

U.S. Environmental Protection Agency, 2009, National primary drinking water regulations: EPA 816-F-09-004, 6 p. Portable Document Format (PDF). [*http://water.epa.gov/drink/contaminants/upload/mcl-2.pdf* accessed October 17, 2012].

U.S. Geological Survey, 2012, Water science glossary of terms: *http://water.usgs.gov/water-basics_glossary.html (*accessed December 15, 2012).

——— 2013, State Geologic Survey Mapping (STATEMAP) Component of the National cooperative Geologic Mapping Program: *http://ncgmp.usgs.gov/about/statemap.html (*accessed February 27, 2013).

Vengosh, Avner, Warner, Nathaniel, Osborn, Stephen, Jackson, Rob, 2011, Elucidating water contamination by fracturing fluids and formation waters from gas wells: Integrating isotopic and geochemical tracers: *in* Proceedings of the technical workshops for the hydraulic fracturing study: chemical and analytical methods, p. 81-83: *in* Proceedings of the technical workshops for the hydraulic fracturing study: chemical and analytical methods: U.S. Environmental Protection Agency, EPA 600/R-11/066, May 2011, 115 p.

Wilde, F. D., Radtke, D. B., Gibs, Jacob, and Iwatsubo, R. T., eds., 2004 with updates through 2009, Processing of water samples (version 2.2): U.S. Geological Survey Techniques of Water-Resources Investigations, book 9, chap. A5, April 2004, *http://pubs.water.usgs.gov/twri9A5/* (accessed October 2, 2012).

Williams, J.H., 2010, Evaluation of well logs for determining the presence of freshwater, saltwater, and gas above the Marcellus Shale in Chemung, Tioga, and Broome Counties, New York: U.S. Geological Survey Scientific Investigations Report 2010–5224, 27 p. (*http://pubs.usgs.gov/sir/2010/5224/*).

Williams, J. H., and Conger, R. W., 1990, Preliminary delineation of contaminated water-bearing fractures intersected by open-hole bedrock wells: Ground Water Monitoring Review, v. 10, no. 4, p. 118-126.
Williams, J. H. and Eckhardt, D. A., 1987, Groundwater resources of the Berwick-Bloomsburg-Danville area, east-central Pennsylvania: Pennsylvania Geological Survey Water Resources Report 68, 89 p.
Williams, J. H., and Johnson, C. D., 2004, Acoustic and optical borehole-wall imaging for fractured-rock aquifer studies: Journal of Applied Geophysics, v. 55, Issue 1-2, p. 151-159. Portable Document Format (PDF). (*http://water.usgs.gov/ogw/bgas/publications/JAG_2004/JAG_2004.pdf*).
Williams, J. H., Taylor, L. E., and Low, D. J., 1998, Hydrogeology and groundwater quality of the glaciated valleys of Bradford, Tioga, and Potter Counties, Pennsylvania: Pennsylvania Geological Survey, 4th ser., Water Resources Report 68, 89 p.
Young, S. C., and Pearson, H. S., 1995, The electromagnetic borehole flowmeter - Description and applications: Ground Water Monitoring and Remediation Review, v. 15, no. 4, p. 138-146.
Zoback, M.L. and M.D, Zoback, 1980, State of stress in the conterminous United States, J. Geophysical Research, 85, 6113-6156.

APPENDICES

All appendix material is located in accompanying folder.